Use of measurements and a canopy exchange model to analyse coniferous forest carbonyl sulphide exchange processes for inferring GPP

Author: Leon Casse

Supervisors: Laurens Ganzeveld & Linda Kooijmans

May 8th, 2020

MSc thesis Meteorology and Air Quality Group

Wageningen University and Research

Abstract

A proper understanding of the CO_2 vegetation sink is required if we want to correctly estimate its contribution to the carbon cycle. The use of carbonyl sulphide (COS) is a relatively new method used for inferring GPP (or CO_2 uptake) which is based on the similarity in stomatal uptake between the two tracers. In this study measured and simulated COS, CO_2 and O_3 mixing ratios and ecosystem fluxes for the boreal forest site Hyytiälä (Finland) were used to improve the understanding of in-canopy processes on COS and to arrive at a representative simulated GPP. This was done using a multi-layer canopy exchange model (MLC-CHEM) considering the stomatal and non-stomatal processes influencing the COS exchange. The processes analysed consist of the influence of entrainment and turbulent mixing on in-canopy COS mixing ratios, the contribution of the soil as a COS sink, the importance of stomatal and internal conductance for COS and CO_2 uptake, and the potential impact of COS uptake by wet vegetation surfaces. Finally, the leaf relative uptake (LRU) and GPP estimates based on this COS method are analysed and compared to the measurements. Analysis of u*, COS and O_3 (in-canopy) mixing ratios showed a strong influence of turbulent mixing and entrainment on in-canopy COS mixing ratios in the early morning. A sharp increase in early morning mixing ratios takes place due stable conditions at night in combination with COS uptake by the soil. However, another significant nocturnal sink is required, since the soil is only responsible for about 40% of night-time COS uptake. This additional sink is likely either night-time stomatal opening and/or COS uptake by wet vegetation. It was further found that during the day vegetation is the main sink for COS where its uptake is more limited by the internal resistance than by the stomatal resistance while both have a similar diurnal cycle. This indicates that it is important to simulate the internal COS resistance with a variable diurnal cycle in order to better reproduce the observations. However, the processes behind this cycle are not yet well known resulting in limitations when it comes to simulating this internal resistance. Model simulations were used to observe the potential effect of COS uptake by wet vegetation, showing a potential for considerable COS uptake even at a relatively high wet vegetation uptake resistance of 10^4 s m^{-1}. The COS measurements showed signs that the wet skin fraction could have an influence on COS mixing ratios and deposition velocities, but due to a large variability in other micrometeorological parameters this was hard to analyse. Therefore, more research is required in a controlled environment to be able to observe the effect of wet vegetation independent of other micrometeorological conditions. Finally, a simulated LRU was obtained which showed no light dependence in contrast to the measurement inferred LRU, indicating a missing light dependence of CO_2 in the model. The resulting simulated GPP, although close to the measured GPP, is likely incorrect because at this point in time the processes influencing COS are not yet known well enough to accurately implement into the model.

Table of Contents

List of Figures

List of Tables

List of abbreviations

$[CO_2]$	CO_2 mixing ratio
[COS]	COS mixing ratio
$[O_3]$	O_3 mixing ratio
CA	Carbonic anhydrase
F_{CO2}	CO_2 leaf flux
F_{COS}	COS leaf flux
F_e	Ecosystem flux
F_s	Soil flux
f_{ws}	Wet skin fraction
g_i	Internal conductance
g_m	Mesophyll conductance
g_s	Stomatal conductance
GPP	Gross primary production
LAD	Leaf area density
LAI	Leaf area index
LRU	Leaf relative uptake
NEE	Net ecosystem exchange
PAR	Photosynthetic active radiation
R_e	Ecosystem respiration
RH	Relative humidity
RuBisCO	Ribulose1,5bisphosphate carboxylase oxygenase
r_i	Internal resistance
r_s	Stomatal resistance
r_{soil}	Soil uptake resistance
r_{ws}	Wet skin uptake resistance
u*	Friction velocity
$V_{d,CO2}$	CO_2 canopy deposition velocity
$V_{d,COS}$	COS canopy deposition velocity
$V_{d,soil}$	Soil COS deposition velocity
V_m	Molar volume
VPD	Vapour pressure deficit

1 Introduction

1.1 Background information

Vegetation is a major component in the global carbon cycle and, together with the oceans, the most important sink for CO_2. It is estimated that the land sink accounts for about 30% of the emitted CO_2 (Le Quéré et al., 2018). Vegetation is thus an important factor in climate change as it has a strong impact on atmospheric CO_2 mixing ratios. Quantifying and understanding the size of the vegetation sink is thus key to assess past and future climate change. The global carbon budget (GCB), which is published every year, contains a summary of all the sources (human emissions and land use change) and sinks (ocean, atmosphere and land) of CO_2 (Le Quéré et al., 2018). Since the GCB of 2017 the global land sink is estimated using models which resulted in an imbalance. This showed that there are still knowledge gaps in the sources and/or sinks of CO_2. One of the largest uncertainties lies in the land sink due to the fact that it is complicated to measure or calculate the CO_2 uptake by vegetation (Le Quéré et al., 2018).

The main reason why CO_2 uptake by vegetation is hard to estimate is because the measured flux represents a net exchange flux being the combination of plant photosynthesis and heterotrophic and autotrophic respiration (R_e). The traditional way to calculate gross primary production (GPP, = CO_2 uptake) is by adding the night-time respiration to the net ecosystem exchange (NEE):

$$GPP = NEE + R_e \qquad (1)$$

This method is based on the assumption that the daytime respiration resembles the nocturnal respiration. Since respiration depends on temperature and light conditions it can be expected that this assumption does not hold (Reichstein et al., 2005). An alternative to the traditional way of calculating GPP is using carbonyl sulphide (COS) as a proxy for photosynthetic carbon uptake (Asaf et al., 2013; Seibt et al., 2010; Wohlfahrt et al., 2012). COS is, similar to CO_2, taken up by vegetation stomatal exchange but not respired by vegetation, so its uptake can be measured directly (Commane et al., 2015). Using COS as an alternative has the potential of reducing the uncertainty present from inferring GPP from measured CO_2 fluxes. However, using COS to infer GPP is a relatively new method and still needs to be improved.

The major sources for COS are the oceans and anthropogenic emissions, while the most important sink is vegetation (Montzka et al., 2007). Both emissions from the oceans and uptake by vegetation are largest during the summer months but are separated spatially. Sources appear to be more dominant in the southern hemisphere compared to the northern hemisphere as mixing ratios are generally higher in the south (Montzka et al., 2007). Once in the atmosphere, COS is relatively stable giving it a lifetime of around 2-3 years. This is long enough for mixing with the stratosphere, where COS can act as a source for sulphate aerosols (Montzka et al., 2007). Given these sources, sinks and its lifetime, COS mixing ratios are around 500 ppt, which is almost six orders of magnitude lower than the CO_2 mixing ratios. This low mixing ratio makes it a challenge to measure COS mixing ratios and exchange fluxes. However with the recent introduction of laser spectrometer instruments the COS can be measured at 10 Hz with an error of < 10 ppt (Kooijmans et al., 2017).

COS uptake by vegetations is a good proxy for CO_2 uptake because it follows the same pathway into the leaf. Both tracers move from the atmosphere into the leaf through the stomata. However, once inside the leaf the two gases are separated by different chemical reactions and enzymes. CO_2 will combine with Rubisco Biphosphate (RuBP) in the Calvin cycle (catalysed by the RuBisCo enzyme), while COS reacts with water through the enzyme carbonic anhydrase (CA) (Stimler et al., 2010). When simplified the two reactions are as follows:

$$CO_2 + H_2O + (light) \xrightarrow{RuBisCo} CH_2O + O_2 \qquad (R1)$$

$$COS + H_2O \xrightarrow{CA} H_2S + CO_2 \qquad (R2)$$

The Calvin cycle involving the enzyme RuBisCo is a dark reaction which does indirectly require light for the regeneration of the RuBP. So the reaction of CO_2 is light dependent and will not take place in the dark (Bonan, 2016). The reaction of COS however does not need any light as the enzyme CA catalyses the reaction of COS and H_2O. This is also evident from the fact that COS is also taken up by vegetation during the night when there is incomplete stomatal closure (Stimler et al., 2010). Figure 1 shows a graphical representation of the processes described above. Here it is shown that CO_2 is also formed in the leaf, while the reaction of COS is irreversible (Kesselmeier & Merk, 1993). The fact that the reaction of COS is irreversible results in that there is no respiration of COS by the plants, while CO_2 shows bi-directions exchange (as shown in Figure 1). This particular characteristic of COS uptake and destruction by leaves is one of the reasons why it is potentially a good proxy for photosynthesis, as the measured leaf scale flux reflects the plant uptake through stomata. But in this uptake by stomata also differences in efficiency of the further diffusion and biogeochemical destruction, reflected by the internal conductance for both COS and CO_2, must be considered. For GPP calculations based on COS it is required to take these differences between the uptake of CO_2 and COS into account. Therefore, COS based GPP calculations uses the measured ecosystem COS exchange and corrects this for the difference between leaf scale uptake rate of CO_2 and COS, normalized for their atmospheric mixing ratios (Stimler et al., 2010). The correction factor for the difference in COS and CO_2 uptake is the leaf relative uptake (LRU), which is found to be between 0.7 and 6.2 (see review in Whelan et al., 2018). The COS based GPP and LRU will be discussed in more detail in the method section (section 2.3.6).

Since the use of COS vegetation uptake as proxy for GPP is still a relatively new method it still contains some uncertainties. The idea that vegetation does not emit COS has been questioned by some studies which, besides vegetation uptake, did also find emission of COS from vegetation (Gimeno et al., 2017). Other studies only found COS emissions with COS mixing ratios considerably lower than what is found in the atmosphere, suggesting the presence of a compensation point (Kesselmeier & Merk, 1993) above which there is uptake and blow which there are emissions or a threshold concentration with a zero COS flux (Stimler et al., 2010). Other uncertainties are associated with soil uptake or emissions. Often the soil is a sink for COS, however with higher temperatures the soil can turn into a source for atmospheric COS (Kaisermann et al., 2018). The fact that there is a soil flux for COS, which can be both positive and negative, poses a limitation to this method of using COS uptake by vegetation to infer GPP and requires adjusting for this soil term when upscaling to ecosystem fluxes. The mechanisms behind the soil flux are not yet completely understood. It has been suggested that both biotic and abiotic processes in the soil results in the uptake or emission of COS. Finally, given that COS decomposition by CA involves the dissolution of COS (Stimler et al., 2010), it raises the question whether vegetation wetness might also affect COS ecosystem fluxes (Campbell et al., 2017). COS has a relatively low solubility, comparable to the solubility of O_3 and CO_2. However, for O_3 a relatively large wet vegetation sink is present (Altimir et al., 2006) indicating the potential for COS uptake by wet vegetation.

In recent years an increasing amount of research has been done on the COS exchange with vegetation and soil. The research is based on measurements as well as model data performed at regional to global scale (Whelan et al., 2018). For this study a canopy exchange model was used to simulate the COS mixing ratio and fluxes on a canopy scale which was then compared to measured data from Hyytiälä, Finland. The use of a canopy scale model can simulate processes happening on a relatively small scale from the leaf- up to the canopy scale, providing new insights into the atmosphere-biosphere-land interactions of COS.

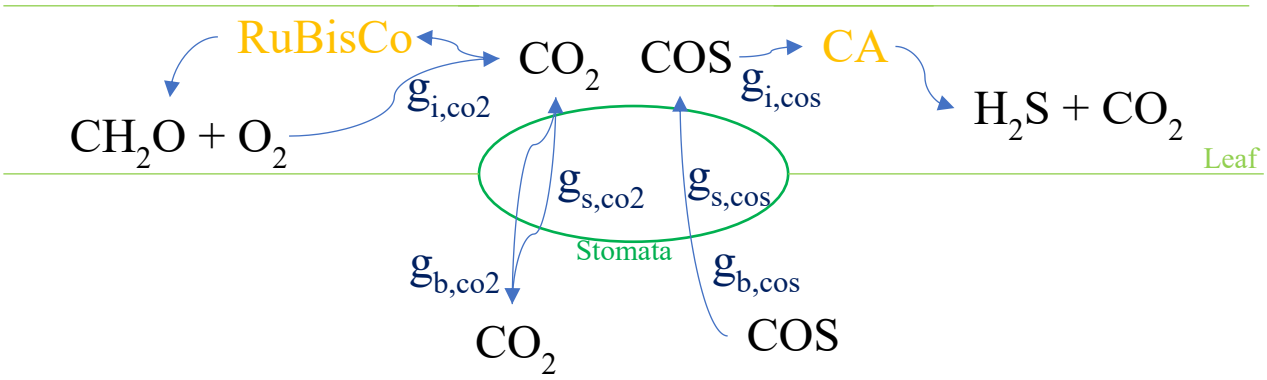

Figure 1: Overview of processes influencing COS and CO_2 fluxes from vegetation. Also shown are the boundary layer, stomatal and internal conductance (g_b, g_s and g_i respectively).

1.2 Research objective

There are still uncertainties in the quantification of sources and sinks of COS and thus more research is still required on this subject (Whelan et al., 2018). This study will combine model simulations and observations to investigate the processes that are involved in the COS exchange between the atmosphere and biosphere. These objectives help to reach the final goal of obtaining accurate GPP estimates. To this end, measured above- and in-canopy COS fluxes and mixing ratios from the Hyytiälä boreal forest research site in Finland will be compared with those simulated by a multi-layer canopy chemistry exchange modelling system called MLC-CHEM (e.g., Ganzeveld et al., 2002; Yanez-Serrano et al., 2018). This combined measurement-modelling analysis will mainly focus on evaluating stomatal and non-stomatal uptake of COS with the stomatal uptake being determined by the stomatal and internal conductance. The non-stomatal exchange will include assessing the potential role of uptake of COS by leaf- and other surfaces, e.g. as a function of vegetation wetness. In addition, the importance of soil fluxes for COS ecosystem fluxes at this particular site will also be analysed. This should eventually lead to an analysis of the quality of the GPP calculations based on the COS flux compared to that of CO2 fluxes. Further details on the methods and data used for GPP calculations are provided in the method section (section 2.3.6).

1.3 Research questions

For this research multiple research questions were proposed. These research questions are divided in two main research questions with several sub questions. The first one focusses on the comparison between the model simulations and measurements whereas the second main research question discusses the overall suitability of using COS for GPP calculations.

How do the model simulated COS fluxes and mixing ratio gradients compare to the measured data at Hyytiälä and what are the main controlling factors?

- How sensitive are in-canopy COS mixing ratios to the soil flux?
- Are there, besides the soil, other nocturnal sinks (or sources) for COS and if so, what are they?
- How does the simulated stomatal and internal conductance from the MLC-CHEM model compare to measured stomatal and mesophyll conductance?
- How do the simulated COS mixing ratios in the canopy compare to the measured COS mixing ratios during a diurnal cycle and during an entire growing season?
- How different is the uptake of COS for wet and dry vegetation?

How different are the COS based GPP estimates compared to NEE based GPP estimates using flux measurements and a canopy model?

- How does the simulated COS based GPP compare to the GPP inferred from CO_2 fluxes during a diurnal cycle and during an entire growing season?
- How does a model based LRU compare to the LRU based on the measurements?

2 Methods

2.1 Measurements

CO_2 and COS mixing ratio, and eddy covariance (EC) measurements were performed at the Hyytiälä measurement station. Here a measurement tower is located where measurements are performed at different heights within and above the boreal forest canopy (at 0.5, 4, 14, 23 and 125 meters). The site is located in the south of Finland (61°51N, 24°17E) within a pine forest dominated by the Scots pine (Pinus sylvestris) (Kooijmans et al., 2017). The height of the vegetation is around 17 meters and relatively uniform around the measurement site. For more details regarding canopy structure see section 2.2. Micrometeorological, tracer mixing ratios and ecosystem fluxes are measured with high frequency but will be analysed as hourly averaged measurements for the period of June until and including October 2015. Measurements on branch COS and CO_2 fluxes were performed in 2017 as well as measurements on COS internal and stomatal conductance. Besides the CO_2 and COS measurements many more parameters are measured at Hyytiälä. This includes mixing ratio and flux measurements of more chemical substances and meteorological data. The meteorological data as well as tracer mixing ratios above the canopy were used as input for the model and are summarized in Table 1. It can be seen that two different measurements of COS mixing ratios, one at an hourly resolution whereas and another being a seasonal cycle without a daily cycle used when the hourly data is missing.

Table 1: Measured parameters used as model input

Parameter:	**Frequency of measurement**	**Elevation above surface of measurement (m)**
Surface/Canopy temperature (K)	Hourly	16.8
Air temperature (K)	Hourly	125
Soil temperature (K)	Hourly	0 to -0.06
Windspeed (m s^{-1})	Hourly	33.6
Friction velocity (m s^{-1})	Hourly	-
Pressure (mb)	Hourly	180 (above sea level)
Net Radiation (W m^{-2})	Hourly	67
Precipitation (mm hr^{-1})	Hourly	18
COS mixing ratio (ppt)	Seasonal cycle (hourly average)	125
COS mixing ratio (ppt)	Hourly	125
CO_2 mixing ratio (ppm)	Hourly	125
O_3 mixing ratio (ppb)	Hourly	125
Relative humidity (0-1)	Hourly	16.8

2.2 Model

The model used for this study is the Multi-Layer Canopy CHemical Exchange Model (MLC-CHEM) which is a canopy model, modelling the source and sink processes taking place inside and just above the canopy, as well as the turbulent transport which ultimately determines the canopy top fluxes. The model has been applied previously in many site-scale analyses of atmosphere-biosphere exchange

processes having demonstrated that ecosystem fluxes of O_3, NO_x, VOCs and other tracers can be simulated well (e.g., Ganzeveld et al., 2002, 2006; Yanez-Serrano et al., 2018). Processes described in this model are biogenic emission, dry deposition, chemistry and turbulent exchange between the vegetation and atmosphere. The model can be run as a stand-alone version or as a biosphere model within a large-scale model (Ganzeveld et al., 2010). As a stand-alone version the model is particularly useful for analysis of local observations (Yanez-Serrano et al., 2018) but it can also be applied to further implement and evaluate updated representation of the in-canopy processes. In this study the stand-alone version of the model was used with the model being constrained by a selection of observed micrometeorological and tracer mixing ratio measurements in the surface layer for a direct comparison with the measurements from the Hyytiälä measurement station (see Table 1).

At the start of this study the model already contained a basic implementation of COS fluxes using the assimilation and stomatal conductance model A-g_s (Ronda et al., 2001). The A-g_s model simulates stomatal conductance as a function of radiation, temperature, moisture and CO_2 mixing ratio. This stomatal conductance is applied in MLC-CHEM for the representation of canopy layer uptake of all tracers including CO_2 and COS also considering prescribed or inferred uptake resistances for soils, cuticles and wet surfaces as a function of reactivity and solubility of each tracer (Wesely, 1989). However, initial comparisons with observations showed that improvements have to be made in the representation of the internal conductance terms and the representation of the soil flux (which is currently a simple linear approximation), see the results section (Section 3.2).

Model simulations were performed for the same period as the measurements from June until November 2015 with timesteps of 30 minutes. The model uses six canopy layers (with reference heights of 1.4, 4.2, 7.2, 9.9, 12.8 and 15.6 meters) to resolve the tracer mixing ratios and fluxes as a function of the imposed observed micrometeorology and surface layer mixing ratios of several tracers (CO_2, COS, O_3). The observed surface layer mixing ratios were used to force the model simulated mixing ratios towards those observations to consider implicitly the role of advection and entrainment into the growing mixed layer. MLC-CHEM simulates the diurnal change in the depth of the mixed layer as a simple prescribed function using an assumed minimum nocturnal mixed layer depth of 180 meters, an assumed maximum afternoon mixed layer depth of 1500 meters and a simple scaling function to introduce a diurnal cycle. However, this is in this study not relevant because the model simulated surface layer COS, CO_2 and O_3 mixing ratios were constrained by the observed mixing ratios. Considering the simulated and measured ecosystem fluxes it should be noted that the simulated fluxes are canopy top (17 m) fluxes while for the measured fluxes the fluxes are representative for a reference height of 23 m. Finally, Table 2 shows the vegetation characteristics for the measurements site as used by MLC-CHEM (Heiskanen et al., 2012; Rautiainen et al., 2012).

Table 2: Vegetation characteristics of the measurement site used by MLC-CHEM

Vegetation type	Coniferous forest
LAI (m^2 m^{-2})	2.8
Canopy height (m)	17
Forest fraction (0-1)	1
Canopy layers	6
Leaf area density (LAD) profile (0-1)	Uniform - (LAD per layer = $\frac{1}{6}$)
Roughness length for momentum (z_m) (m)	1.4

2.3 Data analysis

During this research the data from the measurements was compared with the model output. Generally, besides comparing simulated and observed ecosystem COS fluxes, measured and simulated COS mixing ratios at a height of 4 meters were used for comparison given that for this height the model and measurement heights were similar. When different levels are used this will be mentioned separately. To answer the research questions the analysis has been divided into several sections. The methods and model simulations used are described below.

2.3.1 Soil fluxes

The soil can be an important sink but also potentially a source for COS. Therefore, it is an important parameter to take into account when modelling the COS fluxes. Analysis of measured COS soil fluxes was done to identify its importance. A previous study by Sun et al., (2018) analysed the same soil data for the same period as was studied in this research, therefore data from this paper will be another source of information on the soil fluxes.

Soil flux measurements and COS mixing ratios at 0.5 meters were used to calculate the soil COS deposition velocity ($V_{d,soil}$):

$$V_{d,soil} = \frac{F_{s,COS}}{[COS_{0.5}]} * V_m \qquad (2)$$

with $F_{s,COS}$ being the soil COS flux measured with soil chambers, $[COS_{0.5}]$ is the COS mixing ratio at 0.5 meters and V_m is the molar volume (here assumed to be a constant of 0.023). Using the $Vd_{s,COS}$ the COS uptake resistance of the soil ($r_{soil,COS}$) could be calculated for use in the model.

$$r_{soil,COS} = \frac{1}{V_{d,s,COS}} \qquad (3)$$

This representation of the soil COS flux in MLC-CHEM using a measurement inferred soil uptake resistance implies that solely soil COS deposition is being simulated. Soil CO_2 fluxes are usually emissions and were simulated in a different way. The soil CO_2 flux ($F_{s,CO2}$ in molecules m^{-2} s^{-1}) is calculated using the following equation:

$$F_{s,CO2} = 1 * 10^{-6} * \left(-1.0065 + \exp\left(0.1300 * (T_{soil} - 273.15)\right)\right) * N_a \qquad (4)$$

with T_{soil} being the soil temperature and N_a is the Avogadro constant. This function for the soil CO_2 flux was derived from the measurements at Hyytiälä where the soil CO_2 fluxes were measured.

Further analysis of the correlation between the measured soil COS flux and soil temperature and moisture was performed using Pearson and Spearman correlations. The Pearson correlation is used as a measure for the linear correlation between two variables while the Spearman correlation is used as an indicator for non-linear correlation. Both methods calculate the correlation by dividing the covariance of the two variables by the product of the standard deviation of both variables (Pearson, 1895; Spearman, 1904). Correlation values between -1 and 1 can be found with -1 being perfect negative correlation, 1 a perfect positive correlation and 0 means no correlation.

Finally, these simulations were compared to the soil fluxes found in the measurements as well as with the ecosystem fluxes to observe the contribution of soil uptake on these ecosystem fluxes. Since simulated soil COS fluxes were not available in the diagnostic output of the model the night-time canopy-top COS fluxes were used as an indication of the simulated soil fluxes.

2.3.2 Stomatal conductance

MLC-CHEM uses the A-g_s model to simulate stomatal conductance as well as the CO_2 mesophyll (or internal) uptake resistance considering differences between C3 and C4 vegetation (Ronda et al., 2001). For MLC-CHEM two separate vegetation classes were included; coniferous forest and tropical forest

with adjusted parameters more representative for these types of vegetation. During this study the coniferous forest vegetation type was used in A-g_s. A misrepresentation of the simulated stomatal conductance by A-g_s will results in incorrect CO_2 and COS fluxes. Therefore, the simulated stomatal conductance is compared with measured stomatal conductance using measurement data of 2017 as no data was available for the 2015 period. Since data of a different period was used, this assessment of the quality of the simulated stomatal conductance could only be performed in terms of the magnitude and not the daily trend.

The measured data from 2017 provided stomatal conductance (g_s) for COS, while the A-g_s model output gives g_s values for H_2O which are converted to COS and CO_2 stomatal conductance ($g_{s,COS}$ and $g_{s,CO2}$ respectively) by adjusting for their difference in diffusivity relative to H_2O.

Besides the stomatal conductance, the mesophyll (or internal) conductance (g_m or g_i) is an important term concerning CO_2 and COS uptake. Internal conductance of COS was inferred from the measurements of 2017, while the CO_2 mesophyll conductance was simulated by the model (using the data of 2015). The internal conductance for COS ($g_{i,COS}$) was inferred according to Equation 5 (based on: Kooijmans et al., 2019):

$$g_{i,cos} = \frac{F_{cos} * g_{s,cos}}{F_{cos} + g_{s,COS} * [COS]} \qquad (5)$$

With F_{COS} being the leaf-scale COS flux, $g_{s,COS}$ is the stomatal conductance for COS and [COS] is the atmospheric COS mixing ratios. The $g_{i,COS}$ was then compared to the simulated $g_{m,CO2}$ to assess its importance for the COS flux as well as to incorporate it into the model.

2.3.3 Mixing ratio trends

Previous studies found diurnal cycles in COS mixing ratios that are opposite to in-canopy CO_2 mixing ratios. Where CO_2 mixing ratios decrease during the day the COS mixing ratios increase (Montzka et al., 2007). This characteristic is used for analysing whether the COS implementation in the model is correct. Therefore, the measured daily average mixing ratios are compared with the modelled mixing ratios. This comparison will give a good initial idea about processes taking place in the canopy.

To get a better understanding of the in-canopy processes and their impact on COS (and CO_2) exchange we also included a combined COS-O_3 analysis. This is based on the observation that COS and O_3 atmosphere-biosphere exchange share some canopy processes such as stomatal uptake and, potentially, removal by soil. Consequently, similarities and differences between COS and O_3 mixing ratios indicate what kind of processes are taking place. Processes that were considered are mixed layer dynamics, uptake by wet vegetation and turbulent mixing between the mixed layer and the canopy layers. Unfortunately, a combined COS-O_3 analysis of ecosystem fluxes cannot be included since there are no O_3 flux measurements available at Hyytiälä for 2015. Further, a study of the influence of turbulence on COS mixing ratios is performed as it could potentially have a considerably impact on its diurnal cycle and mixing of the above- and in-canopy air influencing the variation with height. Therefore, the model simulations have also been constrained by the measured friction velocity (u*).

2.3.4 Uptake by wet vegetation

The importance of COS uptake by wet vegetation has seen little to no research before. In this study we will analyse whether the wet vegetation potentially has an impact on (mostly night-time and early morning) COS mixing ratio and fluxes within the canopy. Since there are no measurements available regarding vegetation wetness (f_{ws}) at Hyytiälä, this feature is analysed using the MLC-CHEM simulated fraction of wet vegetation. The model uses a simple empirical relation using measured relative humidity (RH):

$$f_{ws} = 1 - \frac{RH - 0.55}{0.35} \quad (For\ 0.55 \leq RH < 0.9)$$
$$f_{ws} = 1 \quad (For\ RH \geq 0.9) \qquad (6)$$
$$f_{ws} = 0 \quad (For\ RH < 0.55)$$

The inferred f_{ws} was then used to analyse the impact of vegetation wetness on COS mixing ratios within the canopy. This is done by observing whether a correlation is present between the f_{ws} and COS, CO_2 and O_3 mixing ratios as well as with COS and CO_2 deposition velocities ($V_{d,cos}$ and $V_{d,CO2}$ respectively). Canopy scale deposition velocities are calculated by dividing the fluxes of a tracer by the mixing ratios just above the canopy top:

$$V_{d,tracer} = \frac{F_{e,tracer}}{[tracer_{23}]} * V_m \qquad (7)$$

where "tracer" can be either COS or CO_2 and [$tracer_{23}$] is the COS or CO_2 mixing ratio at 23 meters, respectively. These are the mixing ratio measurement closest above the top of the canopy. For the simulations there is no data at 23 meters and therefore a height of 81 meters was used as it is the only point above the canopy available from the model output. Deposition velocities are included in this evaluation of the effect of canopy wetness rather than comparing ecosystem fluxes to focus on removal efficiency.

Next to correlations between the tracers and f_{ws} we also looked at the diurnal trend of COS, CO_2 and O_3 under high and low f_{ws} conditions. Average COS, CO_2 and O_3 diurnal mixing ratios for the entire studied period were plotted and compared with the daily average mixing ratios when f_{ws} is larger than 0.9 or less than 0.1 for different heights in the canopy.

2.3.5 Ecosystem fluxes

For this study, the term ecosystem fluxes refers to the measured and simulated atmosphere-biosphere exchange fluxes on a relatively small scale (i.e. the footprint from eddy-covariance measurements at Hyytiälä). Measured time-series and diurnal trends in COS ecosystem fluxes were compared with those simulated providing insight into the model's performance as well as the temporal variability in fluxes.

Besides a detailed comparison of COS fluxes, we also included a direct comparison of the simulated and observed CO_2 fluxes. This is done to validate whether the model is working correctly in respect to stomatal conductance from the A-g_s model. Incorrect CO_2 fluxes can point to an incorrect stomatal conductance which also influences the COS uptake.

2.3.6 GPP estimates

Finally, GPP calculations were performed for the model and this will be compared with the already calculated GPP from the measurements. This is done both using the traditional NEE based method shown in Equation 1 as well as using the COS based approach which will be described in more detail here. Equation 8 shows how the GPP is calculated from COS flux measurements (GPP_{COS}):

$$GPP_{COS} = \frac{F_{e,COS}}{LRU} * \frac{[CO_2]}{[COS]} \qquad (8)$$

where LRU is the leaf relative uptake, a function of the ratio between the vegetation uptake velocities of COS and CO_2 (Sandoval-Soto et al., 2005). LRU can be calculated with Equation 9:

$$LRU = \frac{F_{COS}}{F_{CO2}} * \frac{[CO_2]}{[COS]} \qquad (9)$$

with F_{COS} and F_{CO2} respectively the COS and CO_2 leaf flux, [CO_2] and [COS] are respectively the atmospheric CO_2 and COS mixing ratio and $F_{e,COS}$ is the ecosystem COS flux (Kooijmans et al., 2019). For the model output no leaf scale fluxes are available, therefore the leaf scale COS and CO_2 fluxes were estimated by dividing the ecosystem fluxes with the LAI (2.8).

The GPP calculated from the measurements from the study of Kooijmans et al. (2019) uses a light dependent LRU to calculate the GPP under different light conditions. The light dependent LRU was based on measured leaf and ecosystem scale COS and CO_2 measurements and resulted in a good fit with the following equation: LRU = 607.26/PAR + 0.57 (See appendix of Kooijmans et al., 2019). This LRU based on measurements at Hyytiälä was applied to the modelled fluxes to compare the simulated GPP with the measured GPP. Next to this a new LRU was calculated based on the simulations using the median value found from applying Equation 9 on the simulated data. This results in the use of two different LRU values to calculate GPP for both the measured and simulated fluxes (so 4 different GPP estimates), which can be compared to the NEE based GPP estimate to observe if the model can represent the CO_2 uptake well and to see if it can improve the measurement inferred LRU.

3 Results

In this section the results of the data analysis are described in order to answer the research questions. First the simulated and measured COS fluxes and in-canopy mixing ratios will be discussed using the final (default) model settings. Next, the role of important stomatal and non-stomatal processes for the fluxes and in-canopy mixing ratios will be analysed. Finally, we will infer the GPP from both the measurements and simulations using the traditional NEE based method as well as with the use of COS.

3.1 Default simulations

During this study changes were made to the MLC-CHEM model to improve its representation of the COS (and CO_2) fluxes (see Appendix A for changes implemented in the model). The results here show the simulated ecosystem fluxes and in-canopy mixing ratios using the final model settings used during this study and compares them to the measurements. These settings use no night-time stomatal opening, no uptake of COS by wet vegetation surfaces a soil uptake resistance of 5100 s m^{-1} and a variable internal COS resistance ($r_{i,COS}$) obtained by scaling it to the stomatal COS resistance ($r_{s,COS}$). More details about these settings and how they were derived will be discussed in section 3.2.

3.1.1 Trends in in-canopy COS mixing ratios

Diurnal cycles and time series of COS and CO_2 were studied to better understand and quantify the role of in-canopy processes influencing especially the COS mixing ratios and ecosystem exchange fluxes. Figure 2 shows the monthly mean diurnal measured and simulated COS and CO_2 mixing ratios at two different heights (i.e. 4 and 14 meters for the measurements and 4.2 and 12.8 meters for the simulations) for July and October 2015. Here it can be seen that for the measurements in both July and October, night-time in-canopy COS mixing ratios are relatively low, while during the day they increase. This diurnal trend in COS mixing ratios is opposite to the trend that can be found for CO_2, which shows lower mixing ratios during the day. For both COS and CO_2, the diurnal variations in mixing ratios are much larger in July than in October, due to the difference in vegetation activity between these months.

When comparing both the COS and CO_2 simulated and measured mixing ratios it was found that for both tracers, though the magnitude of the simulated mixing ratios is close to the measured one, the diurnal cycle is generally not simulated correctly. For COS the measured mixing ratios start increasing earlier than the simulated mixing ratios most clearly seen in July while simulated mixing ratios also remain too high during the night. Simulated CO_2 mixing ratios are generally too low both in July and October. During July the measured and simulated diurnal cycle is relatively comparable except that the CO_2 mixing ratios start increasing earlier for the measured data in the afternoon. Further, the simulated mixing ratios at 4 meters become lower than at 12 meters while this does not occur in the measured data, indicating a too strong simulated day-time sink close to the soil or too small soil CO_2 emissions.

Figure 3 shows a comparison of the observed and simulated COS and CO_2 mixing ratios at 4 and 14 meters (and 4.2 and 12.8 meters for simulated data) for a two-week period in July (5-20 July). From this figure it can be inferred that COS mixing ratios are generally relatively well simulated although mixing ratios in the early morning are usually too high (as was shown in Figure 2). Simulated CO_2 mixing ratios are generally too low especially during the night, while during the day the simulated CO_2 mixing ratios follow the measured CO_2 relatively well. In the night of the 17th to the 18th of July the simulated COS and CO_2 mixing ratios show very low and high values respectively, while also the measured COS mixing ratios at 4 meters is relatively low. This period is characterised by little turbulence ($u^* < 0.1$ m s^{-1}) which apparently results in night-time COS depletion while CO_2 is building up causing unusually high mixing ratios. The model appears to overestimate the effect of stable conditions on the in-canopy mixing ratios. This result could indicate a role of too large soil exchange fluxes (either uptake for COS or emission for CO_2) or a misrepresentation of mixing conditions with other in- and above-canopy layers. However, since the effect of low u* can be observed for both simulated COS and CO_2 mixing ratios it implies that both soil fluxes are simulated wrong which seems unlikely, so it is more likely that the mixing with in- and above-canopy layers within the model is simulated incorrectly under these conditions.

Following this analysis of the simulated and measured mixing ratios it can be concluded that the model simulations arrive at a relatively good mixing ratio however, the timing between the measurements and simulations are not entirely correct. This could potentially have an influence on the COS and CO_2 fluxes which will be discussed in the next section.

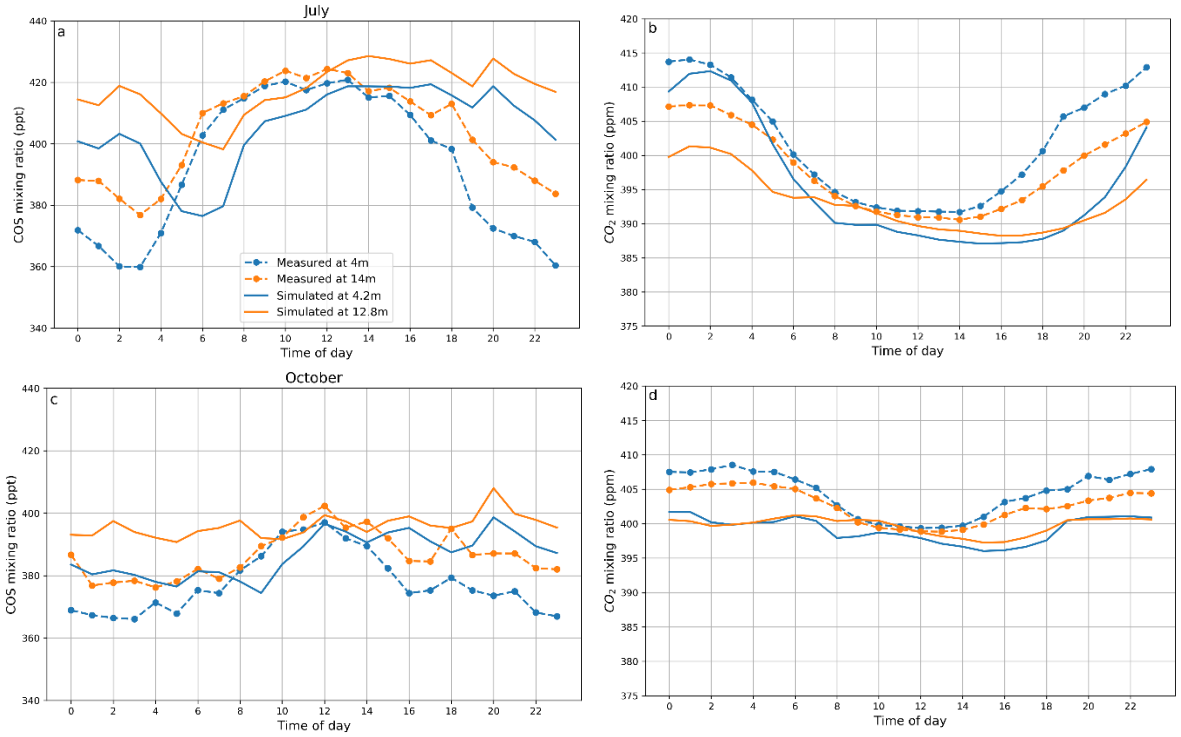

Figure 2: Monthly mean diurnal cycle in measured (dots) and simulated (solid lines) a) COS mixing ratios for July, b) CO_2 mixing ratios for July, c) COS mixing ratios for October and d) CO_2 mixing ratios for October at 4 meters (in blue) and 14 meters (or 12.8 meters for simulated – in orange).

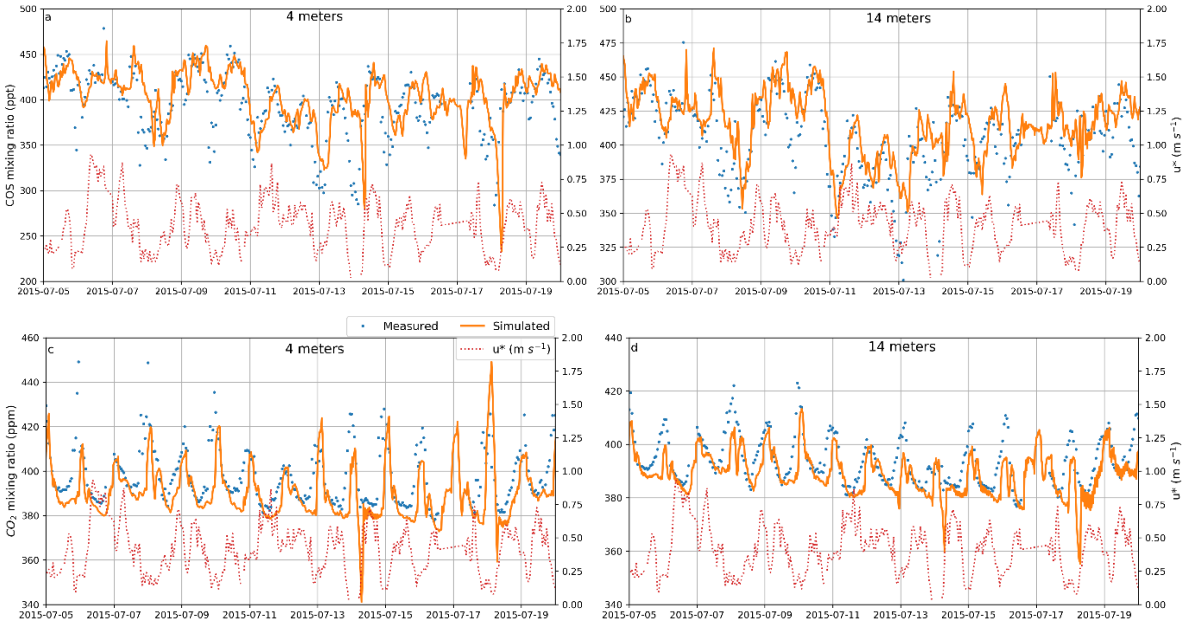

Figure 3: Measured (blue dots) and simulated (orange lines) a) COS mixing ratios at 4 meters, b) COS mixing ratio at 14 meters, c) CO_2 mixing ratio at 4 meters and d) CO_2 mixing ratio at 14 meters for the period of July 5th until July 20th 2015. Red dotted line indicates measured u.*

3.1.2 Flux simulations and deposition velocities

Figure 4 shows the monthly mean diurnal cycle in COS and CO_2 ecosystem fluxes for July and October, where negative values indicate a downward flux and uptake by the forest canopy. Here it is shown that during July the simulated COS flux shows a similar diurnal cycle compared to the measurements, but mainly at night and in the early morning simulated COS fluxes are relatively low. Simulated CO_2 ecosystem fluxes on the other hand show too high values during the night and late afternoon. However, for both the simulated and measured average COS and CO_2 ecosystem fluxes the maximum value, around noon, are relatively comparable and their timing is similar. Only for CO_2 the ecosystem fluxes peak slightly earlier for the measurements than for the simulations possibly due to a stronger vapor pressure deficit (VPD) effect in the measurements. In contrast, the simulated fluxes show no indication of an afternoon decrease in uptake associated with the VPD effect during this period. Further, this VPD effect should then also be visible in measured COS fluxes while this is not observed. A high VPD is usually found during periods of low RH and/or high temperatures resulting in stomata closure to prevent water loss, thereby resulting in lower stomatal uptake for both CO_2 and COS. It may be that the larger uncertainty due to lower precision in measured COS fluxes masks the VPD effect or possibly the faster decrease in measured CO_2 fluxes in the afternoon is caused by another process (e.g. larger soil respiration). The stomatal conductance and VPD effect will be further discussed in Section 3.2.3.

For October the simulated COS fluxes are relatively low compared to the average measured flux, but fluxes are in general around half of the fluxes in July. Night-time COS fluxes appear to be simulated better during October than for July while day-time ecosystem fluxes appear too low in October. Simulated CO_2 ecosystem fluxes have a higher and later peak in October compared to the measured CO_2 flux and both the fluxes in the early morning and later afternoon are too high like they were in July. Night-time simulated CO_2 fluxes appear to agree somewhat better with the observations in October but are still slightly too high (less positive).

It has to be noted that the COS flux measurements show a relatively large spread and a much less consistent diurnal cycle likely due to less precise COS measurements compared to those for CO_2 (Kooijmans et al., 2016). The large spread in the measurements is indicated by the blue shaded area in Figure 4, indicating one standard deviation above and below the average measured COS flux. The

simulated COS ecosystem fluxes are generally found to be within one standard deviation from the measurements while for CO_2 the simulated ecosystem fluxes are frequently found outside this standard deviation except around noon. However, since the large spread is due to less precise COS measurements and as long as this does not result in a bias towards higher or lower measured fluxes it can be assumed that the measured mean is relatively close to the actual conditions. So, although the simulated COS ecosystem fluxes appear better than the CO_2 fluxes, this actually reflects the more precise CO_2 measurements.

Differences between the measured and simulated ecosystem fluxes can be due to all sorts of processes occurring in the canopy which have to be modelled correctly. Most of these processes that can influence the fluxes of COS and CO_2 are further addressed in Section 3.2 as well as in in Section 4. However, another reason for potential differences between the measurements and the simulations is due to different measured and simulated in- canopy COS and CO_2 mixing ratios. In the previous section it could be seen that the measured and simulated mixing ratios do not always agree well mostly due to a difference in timing. This potentially results in different fluxes since these fluxes depend on the mixing ratio gradients which in turn are also affected again by these fluxes. To further analyse the potential explanations for some of the established discrepancies in simulated and observed fluxes we further diagnosed the deposition velocities (V_d) to assess the exchange processes of both tracers within the canopy.

Figure 5 shows the average diurnal $V_{d,COS}$ and $V_{d,CO2}$ for the months of June and October. The values here are mostly positive reflecting deposition, resulting in an opposite but comparable trend to the one found in Figure 4. Despite the fact that the simulated and measured mixing ratios do not always agree well it can be inferred from Figure 4 and 5 that the difference between the measured and simulated V_d is relatively small but showing some comparable discrepancies compared to that what was seen in the comparison of ecosystem fluxes. This means that the same conclusion can be drawn for both Figures. This shows that the differences between the measured and simulated mixing ratios have little effect on their difference in ecosystem fluxes.

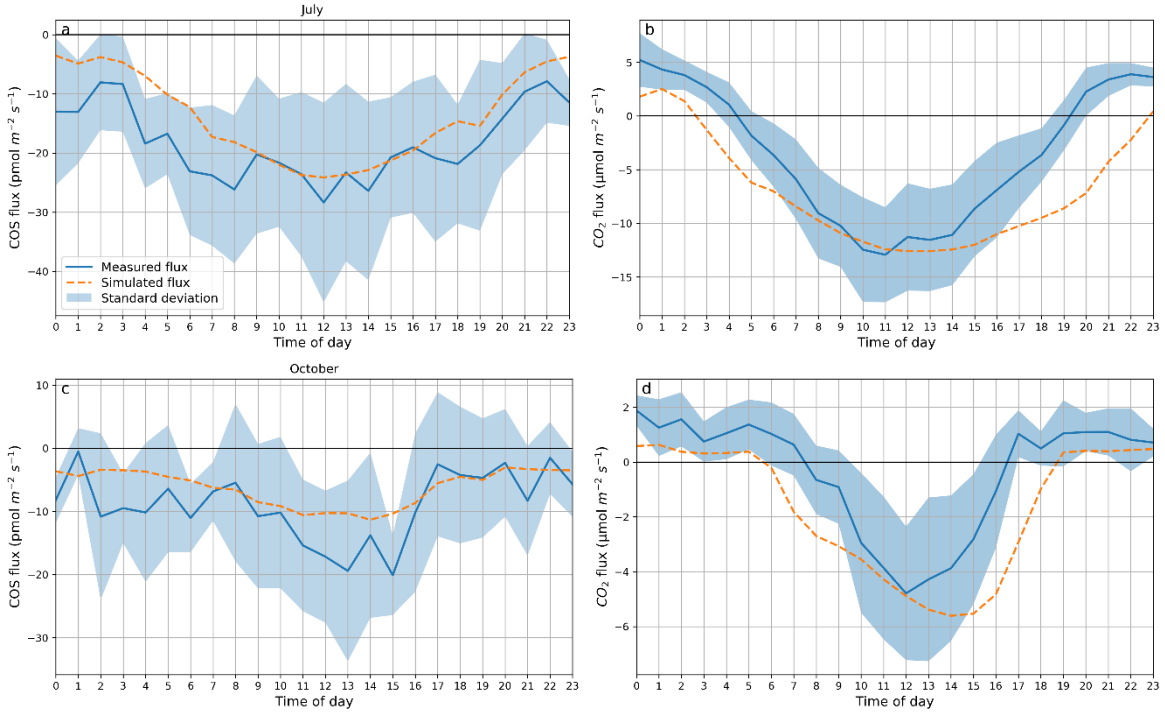

Figure 4: Measured (blue line) and simulated (orange dashed line) average diurnal a) COS ecosystem fluxes for July, b) CO_2 ecosystem fluxes for July, c) COS ecosystem fluxes for October and d) CO_2 ecosystem fluxes for October. With the blue area around the average measured flux curve showing its standard deviation.

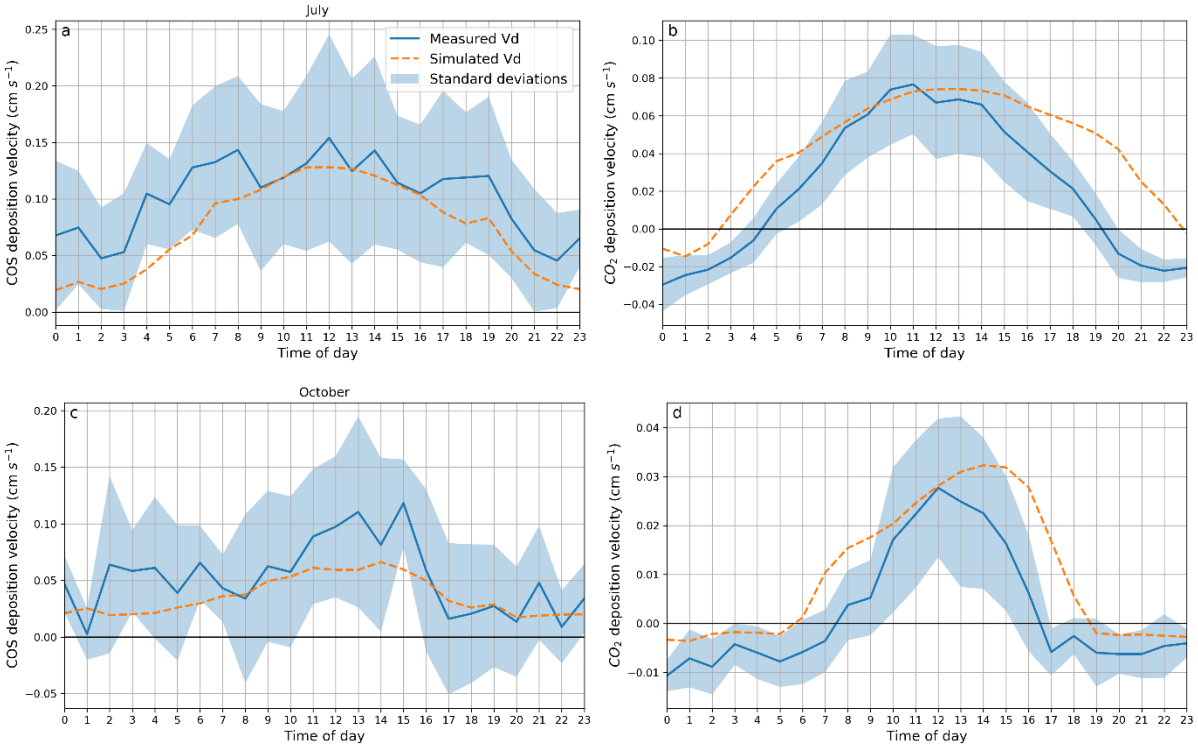

Figure 5: Measured (blue line) and simulated (orange dashed line) average diurnal a) COS deposition velocity for July, b) CO_2 deposition velocity for July, c) COS deposition velocity for October and d) CO_2 deposition velocity for October. With the blue area around the average measured flux curve showing its standard deviation.

3.2 In- and above-canopy processes

In this section we will go further into the specific processes studied during this study. This will be done by comparing different simulation using different model settings and analysing what appears to correspond best with the measurements. The previous section only looked at the final (default) model settings, while here it will be shown what these model settings are and how we arrived at the final settings.

3.2.1 Relations between mixing and COS mixing ratios

In section 3.1.1 it was shown that the diurnal cycle in COS and CO_2 mixing ratios are opposite. Where COS mixing ratios are high during the day, CO_2 has its peak mixing ratios during the night. Here the processes influencing COS and CO_2 mixing ratios will be studied to be able to explain the differences between these tracers. Figure 6 shows the correlation between the COS and CO_2 mixing ratio as a function of u* for both the measured as well as the simulated data for the entire measurement campaign. From this figure it can be inferred that the measured COS mixing ratios correlate stronger with u* (r = 0.566) than the CO_2 mixing ratios (r = -0.377). This also shows that higher u* results in higher COS mixing ratio, while CO_2 mixing ratio are higher for lower u*, however correlation is weak as also lowest CO_2 mixing ratios are found under low u*. The u* in MLC-CHEM is constrained by the measured u*. However, the correlations between u* and COS mixing ratios are less strong in the simulations than for the measured data (r = 0.384) as can also be seen for CO_2 (r = -0.256). This indicates that other processes are more important for simulated COS and CO_2 mixing ratios or that despite imposing the observed u*, turbulent mixing between the surface and canopy layers is not simulated correctly.

The good correlation between COS mixing ratio and u* can arise due to a similar diurnal cycle in COS mixing ratios and u*. Figure 7 shows the average diurnal cycle of the COS and O_3 mixing ratio at 4 meters as well as u* for the entire measurement campaign. Here it can be seen that the diurnal cycle

of these parameters are in good agreement. All three increase in the early morning to find its peak around midday and thereafter decrease again. Both the diurnal cycle in COS and O_3 mixing ratio at 4 meters show the similar pattern as u* indicating that the simulated and observed increase in COS mixing ratios in the early morning are associated with an increase in turbulent mixing in the early morning. This also indicates that the positive correlation between u* and COS mixing ratios (Figure 6) is found due to COS uptake at night (see Figure 4) under stable conditions (low u*). CO_2 on the other hand is emitted at night and therefore CO_2 can build up under the stable conditions explaining its negative correlation with u*. The more stable the conditions are the stronger this depletion and build-up of respectively COS and CO_2 can become. Further, this onset of turbulent mixing also results in the breaking up of the night-time inversion layer and which apparently also affect COS mixing ratios possibly due to either advection or entrainment of the overlaying residual layer.

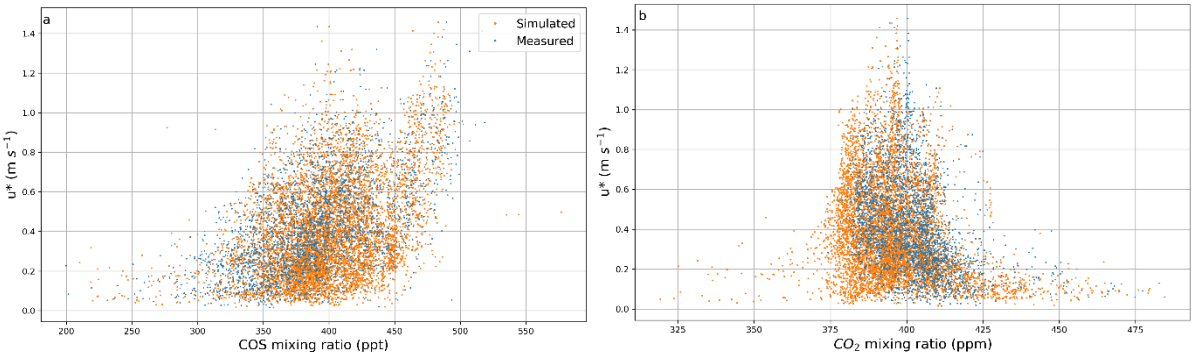

Figure 6: Correlation of u with a) COS mixing ratios and b) CO_2 mixing ratios for both the measurements (blue points) and simulations (orange points) at 4 meters for the entire measurement campaign (June until October 2015).*

Ecosystem exchange of O_3 has seen focus of many studies and therefore more is known about the processes influencing its mixing ratio within the canopy (Aneja et al., 2000; Hastie et al., 1993). Therefore, besides the mean diurnal cycle in O_3 and COS mixing ratios, a timeseries of the two tracers are studied. This is shown in Figure 8 for the period from the 2nd until the 20th of August. It is interesting to observe that the COS and O_3 mixing ratios follow a very similar cycle with high mixing ratios during the day and lower mixing ratios at night as was also seen in Figure 7. This suggests that the mixing ratios of the two tracers are influenced by similar mechanisms controlling these mixing ratios. In previous studies it has been found that O_3 mixing ratios in the early morning strongly depend on the entrainment as the mixed layer grows (Hastie et al., 1993). Observations generally show O_3 depletion during the night, also explained by soil deposition and titration by NO, followed by a sharp rise in O_3 mixing ratios. Hastie et al. (1993), found that during the morning an increase in O_3 mixing ratios of 20 ppb within 2 hours occurred frequently which is around the same magnitude as found during this study. COS mixing ratios frequently rise more than 75 ppt in just a few hours at the same time as the increase in O_3 mixing ratio takes place. This further supports that during the early morning COS

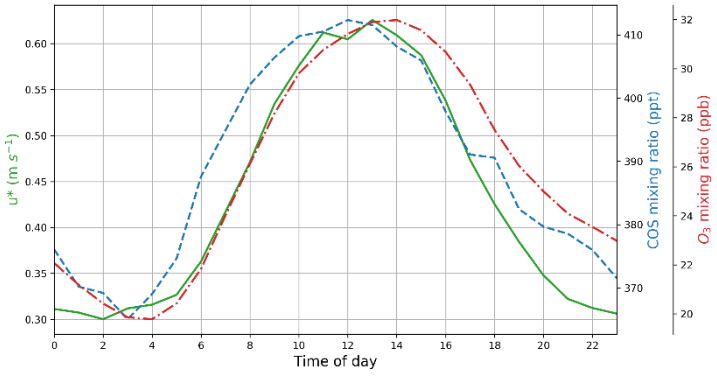

Figure 7: Average diurnal cycle of measured COS mixing ratio at 4 meters (blue dotted line), O_3 mixing ratio at 4 meters (red dotted line) and u (green line) for the entire measurement campaign.*

mixing ratios are also controlled by entrainment of air masses enhanced in COS. Further, both the O_3 and COS are taken up by vegetation and soil during the day explaining their comparable trend during the rest of the day.

Differences between the COS and O_3 mixing ratios are caused by the different exchange processes of the two gases. Where O_3 is also affected by photochemical reactions, COS can be deemed inert on the timescale of surface and boundary layer exchange processes. The role of other in-canopy source and sink processes such as uptake by wet vegetation will be discussed in following sections.

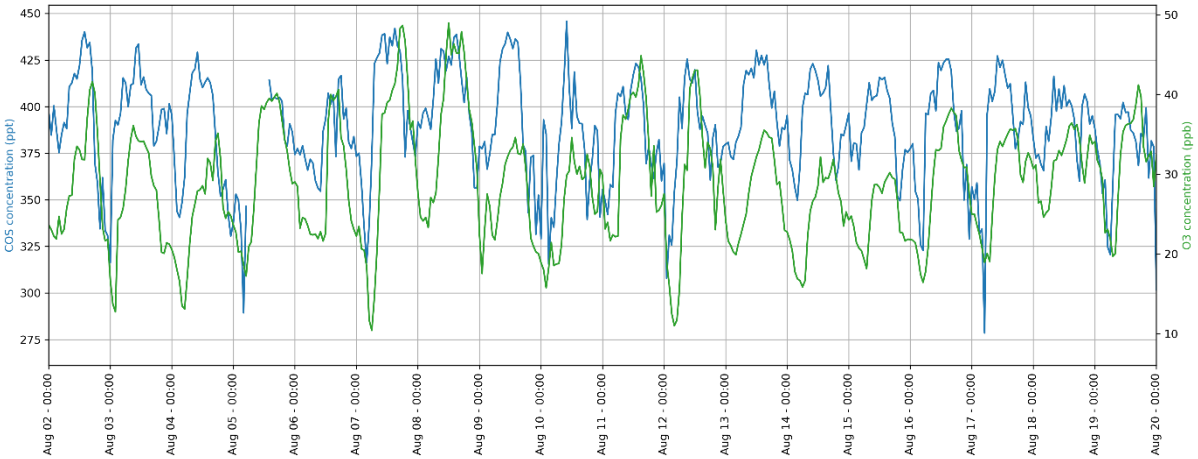

Figure 8: Time series of COS (blue line) and O_3 (green line) mixing ratios for the period of August 2nd until the 20th.

3.2.2 Soil and night-time fluxes

Soil COS exchange was not yet incorporated in the model at the start of this study. Therefore, first an analysis of the measured soil flux was required to assess its importance and to be able to implement it into the model as accurate as possible. Figure 9 shows the average measured soil COS flux found during the measurement campaign (from July until and including October 2015), with negative values indicating COS uptake. During this period the soil always acted as a sink for COS with a mean soil COS flux of -2.8 (±1.0) pmol m^{-2} s^{-1}. Little diurnal variations were present in the average diurnal soil COS flux, however, fluxes appear larger in the early morning and a bit smaller later during the day (Figure 9). Differences in soil fluxes may arise from changes in soil temperature (T_{soil}) or soil moisture (swc) due to their influence on diffusivity of COS through the soil and on microbial activity (Sun et al., 2015; Yang et al., 2019). Figure 10 shows the correlations between the measured soil COS flux and swc and T_{soil}. There is a large spread in COS soil fluxes as a function of the measured range in T_{soil} while regarding the dependence of the COS soil flux on swc it appears to be consisting of two separate regimes. With low swc the soil uptake appears to be higher than with high swc, while for both regimes no clear correlation can be found. Correlations (r values) of 0.261 and 0.276 between respectively the T_{soil} and swc with the soil COS fluxes confirm that correlations are weak.

Using the measurements an $r_{soil,COS}$ was calculated using Equations 2 and 3, arriving at a constant $r_{soil,COS}$ of 5100 s m^{-1} (Sun et al., 2018). Further study of the simulated COS mixing ratio and fluxes is therefore done using this constant

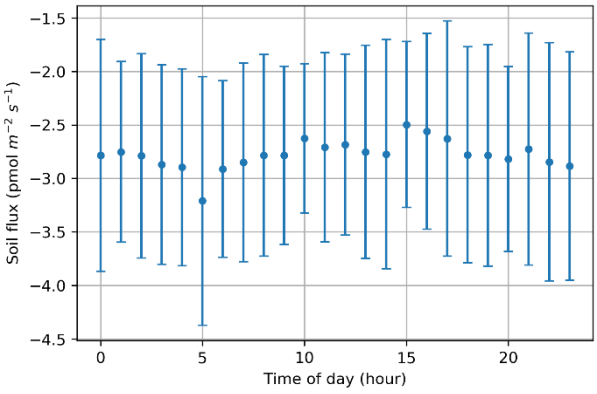

Figure 9: Average measured diurnal cycle of the soil flux at Hyytiälä for the period from June until and including October 2015. The error bars indicate the standard deviation.

$r_{soil,COS}$ in MLC-CHEM. Resulting night-time COS ecosystem fluxes can be seen in Figure 11, where a boxplot of the nocturnal measured and simulated above canopy COS ecosystem fluxes ($F_{e,COS}$) as well as the measured COS soil flux ($F_{s,COS}$) is shown (for July until and including October) with negative values indicating COS uptake. The measured COS soil flux is relatively small and invariable compared to the measured ecosystem flux, while the simulated ecosystem COS flux is close to the measured soil flux. Some of the differences between the measured and simulated night-time $F_{e,COS}$ (and the measured soil flux) may arise from some influence of temperature or soil moisture on the COS fluxes not taken into account by the model using a constant $r_{soil,COS}$. However, it is expected that most of the differences will likely be due to night-time stomatal opening (incomplete stomatal closure) or uptake by wet vegetation surfaces. For the simulations shown in Figure 11 it was assumed that night-time stomatal conductance is virtually zero and water uptake resistance is very high ($r_{ws} = 10^5$ s m^{-1}) to make sure only the soil flux was present at night. It can thus be concluded that on average the model represents the soil flux relatively well but is still missing other uptake processes at night. Next, we will look further into the effect of night-time stomatal conductance on the COS fluxes as well as the potential impact of enhanced uptake by wet vegetation on the night-time COS ecosystem fluxes. This importance and impact of wet vegetation surfaces on diurnal mixing ratio and fluxes will be discussed in more detail in section 3.2.4.

Night-time measured and simulated ecosystem and soil fluxes are shown in Figure 12 for a simulation with a non-zero night-time stomatal conductance and also a simulation with a reduced water uptake resistance (r_{ws}) of 10^4 s m^{-1} (which was initially set to 10^5 s m^{-1}). Both simulations show higher night-time COS ecosystem fluxes than previous simulations and are relatively close to the measured ecosystem flux. The variability in the measured night-time COS ecosystem fluxes is still higher than for the simulated fluxes, while the variability in simulated fluxes is larger with a lower r_{ws} than with the night-time stomatal opening. The simulations with a night-time stomatal opening were performed by assigning a constant g_s value (of $2*10^3$ s m^{-1}) for periods with very low or no incoming shortwave radiation. Therefore, it is not surprising that this simulation gives relatively little variation since invariable night-time g_s will result in little variation in the fluxes. From these results it can be inferred that both processes could explain the difference in night-time soil and ecosystem fluxes while also a combination of the two cannot be ruled out. It is thus not clear what process causes the high simulated night-time fluxes and therefore it is decided to not include the incomplete stomatal closure or a lower wet skin uptake resistance in the final model settings. The individual contribution of stomatal conductance will be further discussed in more detail in the next Section (3.2.3) and uptake by wet vegetation surfaces in Section 3.2.4.

It appears that soil flux is a major sink during the night, however, it is less important during the day. During the night the soil flux is responsible for about 30 to 45% of the total ecosystem flux while during the day 12 to 20% can be attributed to the soil. This shows that when using ecosystem COS fluxes to calculate GPP it is required to correct for the soil flux as this will make a considerable difference, but since the COS soil flux is not very variable over a day it is relatively straightforward to apply this correction. Further, it should be noted that GPP is zero at night due to the lack of light and consequently these features of incomplete stomatal closure or night-time uptake of COS by wet vegetation are not incorporated in the model regarding the GPP calculations. However, the uptake of COS by wet vegetation could also influence day-time mixing ratios and fluxes and will therefore be discussed in a later section.

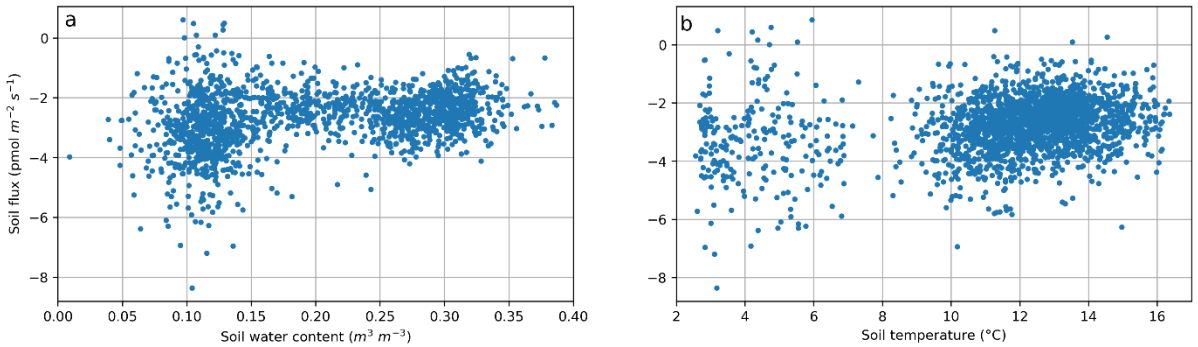

Figure 10: Correlation between soil COS flux and a) Soil water content and b) Soil temperature during the entire measurement campaign.

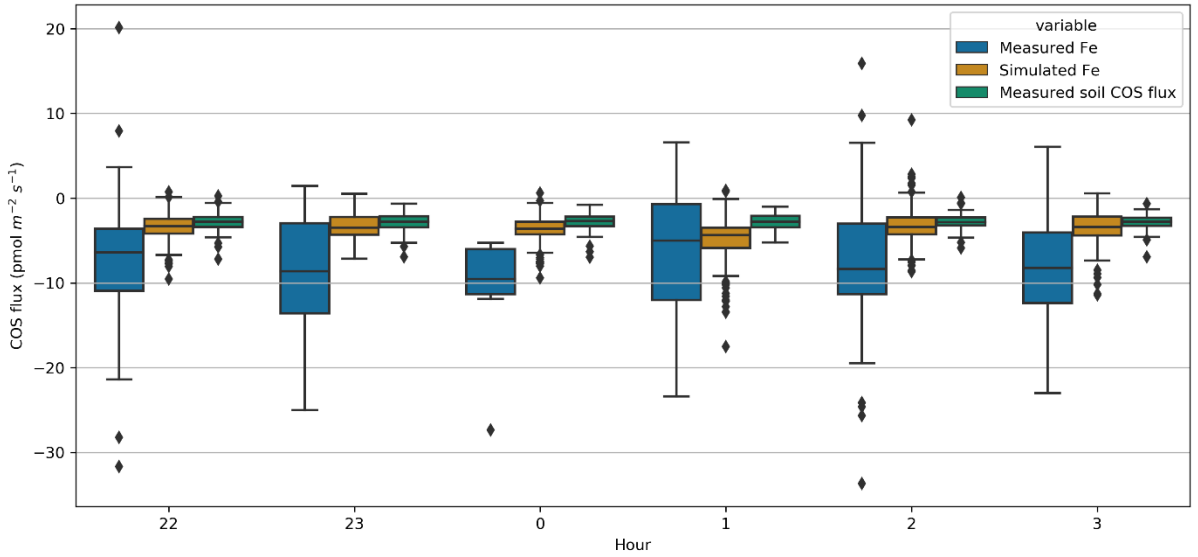

Figure 11: Boxplot of measured (in blue) and simulated (in orange) night-time ecosystem COS fluxes (F_e) and measured soil COS flux (in green) for the period July to October 2015. Negative values indicate uptake of COS.

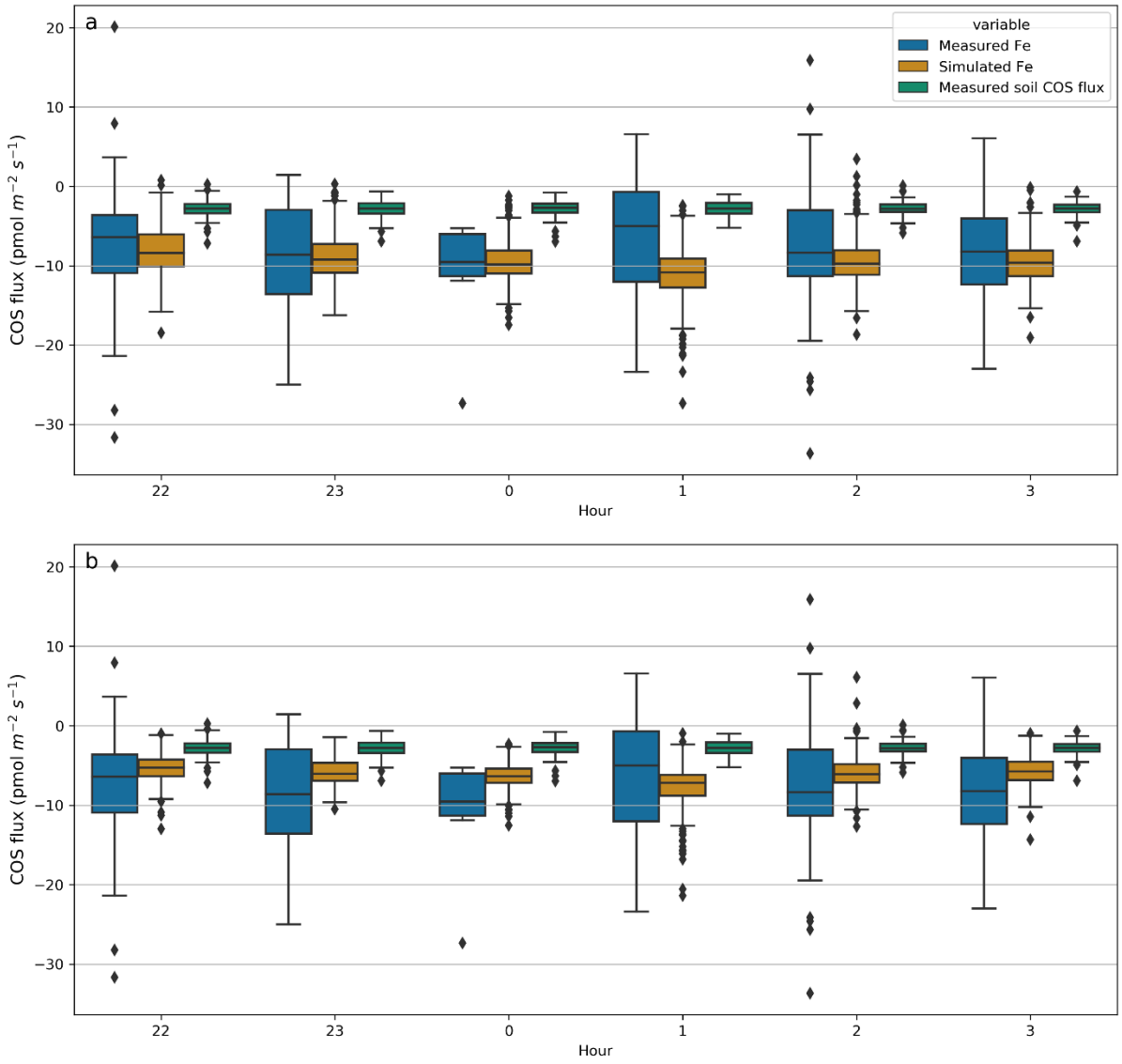

Figure 12: Boxplot of measured and simulated night-time ecosystem COS fluxes (F_e) and measured soil COS flux using an a) r_{ws} of 10^4 s m^{-1} or a b) non-zero night-time g_s for the period July to October 2015. Negative values indicate uptake of COS.

3.2.3 Stomatal and internal conductance

Initially the A-g_s simulated stomatal conductance (g_s) was found to be too high resulting in very large CO_2 and COS fluxes throughout the entire study period. Changes to the A-g_s model were made to modify the model's representation of g_s as well as mesophyll CO_2 conductance ($g_{m,CO2}$) according to values for Scots pine found in literature. First the minimum mesophyll conductance for CO_2 at 25°C was changed from 7 to 1 mm s^{-1}, as this increases both the simulated internal and stomatal resistance, decreasing fluxes considerably. The minimum mesophyll conductance will occur under most optimal conditions for vegetation uptake and was previously found to be 0.9 mm s^{-1} for Scots pine (Linder & Troeng, 1980). Next, the maximum photosynthetic capacity (A_{max}) in the A-g_s model was increased from 0.45 to 1 mg m^{-2} s^{-1} based on two previous studies (Schulze et al., 1994; Wang et al., 1995). The average of these two studies was found to be close to 1 mg m^{-2} s^{-1}. Finally, changes were made in the ratio of internal and ambient CO_2 mixing ratio (C_i/C_a). This A-g_s model parameter was originally set to a value of 0.90, but from Seibt et al. (2010) it was found that for Scots pine a value of 0.71 seems more representative. We selected a value of 0.85, in between the original and the one found by Seibt et al., as this resulted in a simulated stomatal conductance that compared best with the observed stomatal

conductance. An overview of the original values and changes made to the A-g_s model can be found in Appendix B.

Figure 13 shows a time series of the measured leaf scale g_s during June 2017 at Hyytiälä, multiplied with the leaf area index (LAI) of 2.8 to convert it to a canopy scale g_s, as well as the June 2015 simulated canopy scale g_s for the modified A-g_s model. Simulated g_s is generally larger than the measured g_s, mostly later in the day. This is also shown in Figure 14, which shows the average diurnal g_s for the measured and simulated periods. The measured stomatal conductance peaks before midday and decreases gradually after this point, which indicates the potential role of a VPD effect in the afternoon. This is supported by a previous study using the same dataset (Kooijmans et al., 2019). According to the model no or at least a weaker VPD effect is present during June 2015 resulting in a later peak in g_s. Since no measurements for VPD were present for the 2015 period and the A-g_s's model representation of VPD cannot easily be diagnosed in MLC-CHEM, this could not be analysed directly. However, MLC-CHEM diagnostics include an alternative attenuation function for the VPD effect (f_{VPD}) with a value between 0 and 1, with 1 reflecting no VPD effect whereas a value of 0 implies complete stomatal closure. The f_{VPD} for June 2015 rarely decreases below 0.8 and is generally around or above 0.9, indicating only a very minimal influence of VPD on stomatal conductance. Figure 14 shows that the initial early morning increase in simulated and measured g_s agree well, but after a few hours the measured g_s keeps on increasing while the simulated g_s already shows a less strong increase. But then the observed monthly (June 2017) mean maximum g_s of around 0.27 cm s^{-1} is reached at 7AM followed by a continuous decrease whereas the simulated (June 2015) maximum g_s of around 0.32 cm s^{-1} occurs around 1PM. These results might indicate that, despite the comparable onset and increase in the early morning g_s, the simulated g_s might even be underestimated compared to the actual June 2015 maximum g_s at the site as it should increase even more in the early morning. Therefore, the potential maximum stomatal conductance in the afternoon for conditions not limited by VPD is likely higher than the one found in Figure 14. Further, note that measured non-zero night-time g_s values are found whereas the simulated nocturnal g_s is zero. Thus, at this site there is indications of incomplete stomatal closure which could possibly be due to the very short June nights in Hyytiälä resulting in light reaching the vegetation even during most nights.

Besides the stomatal conductance also the internal (or mesophyll) conductance ($g_{i,COS}$) for COS needs to be included in MLC-CHEM. Measurements indicate that $g_{i,COS}$ is more limiting than the $g_{s,COS}$ (Kooijmans et al., 2019), therefore being an important term in simulating COS fluxes. A median $g_{i,COS}$ of around 0.021 cm s^{-1} was found from the measurements, corresponding to a $r_{i,COS}$ of 4700 s m^{-1}. This constant $r_{i,COS}$ is used in the MLC-CHEM simulations. However, MLC-CHEM also allowed the application of a variable $r_{i,COS}$ as a function of $r_{s,COS}$. Figure 15 shows the ratio between the measured $r_{i,COS}$ and the $r_{s,COS}$ for June 2017. This shows that during day-time (indicated by green shaded area) the ratio is relatively constant between 2.5 and 3 with lower values during the night. The mean day-time ratio is 2.6 which is used in MLC-CHEM to consider a variable $r_{i,COS}$. This results in an average $r_{i,COS}$ of 4800 s m^{-1}, and thus close to the average measured $r_{i,COS}$ which was used for the constant $r_{i,COS}$. The result of the simulations with the variable and constant $r_{i,COS}$ is shown in Figure 16, where the average diurnal COS ecosystem flux is shown for the month of July. Here it can be seen that the simulations with a variable $r_{i,COS}$ result in a more representative COS flux compared to the measurements. The simulation with a constant $r_{i,COS}$ remains low throughout the day also missing the observed peak fluxes. The variable $r_{i,COS}$ has nearly no effect on the night-time, early morning and evening fluxes since during these periods stomatal conductance is very low and therefore more limiting. The variable $r_{i,COS}$, calculated from $r_{s,COS}$, was used for the final model settings since this gave the best results. It is, however, still not resulting in an optimal comparison since the daily cycle of the $r_{i,COS}$ and $r_{s,COS}$ are not

the same and resulting fluxes are often underestimated except for the hours around midday. It could be that this underestimation in simulated COS fluxes arises due to the presence of another sink, but this sink has so far not been found in previous studies. Finally, also the simulated $r_{s,COS}$ might be different than the actual diurnal cycle in $r_{s,COS}$ at Hyytiälä as discussed previously which would result in an incorrect $r_{i,COS}$ and a misrepresentation of the fluxes.

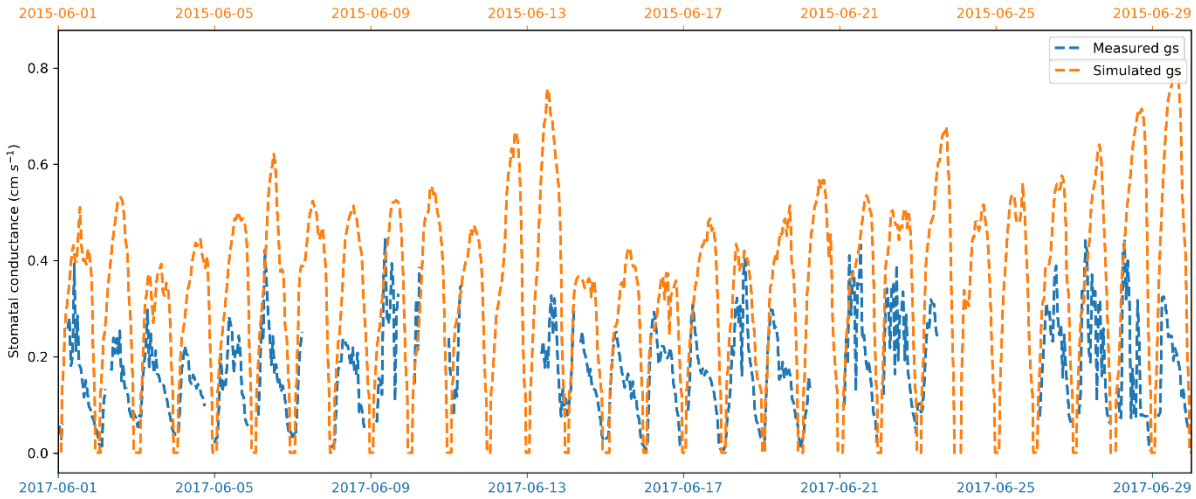

Figure 13: Measured (in blue – data for 2017) and simulated (in orange – data for 2015) stomatal conductance for the month of July.

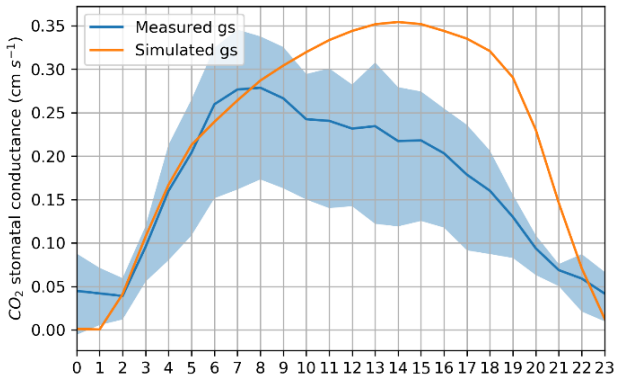

Figure 14:Monthly mean diurnal cycle in measured g_s for June 2017 (in blue) including standard deviation (blue shaded area) and simulated gs for June 2015 (in orange).

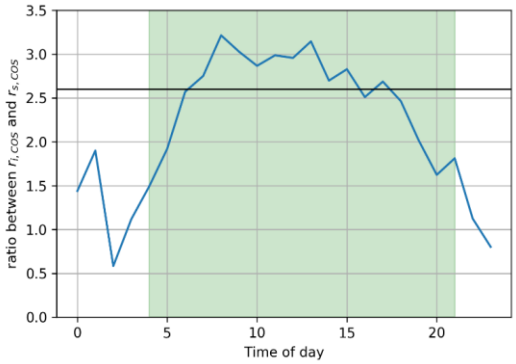

Figure 15: The ratio between average measured June $r_{s,COS}$ and $r_{i,COS}$. The green area shows the day-time while the black horizontal line indicates a value of 2.6 (mean day-time ratio).

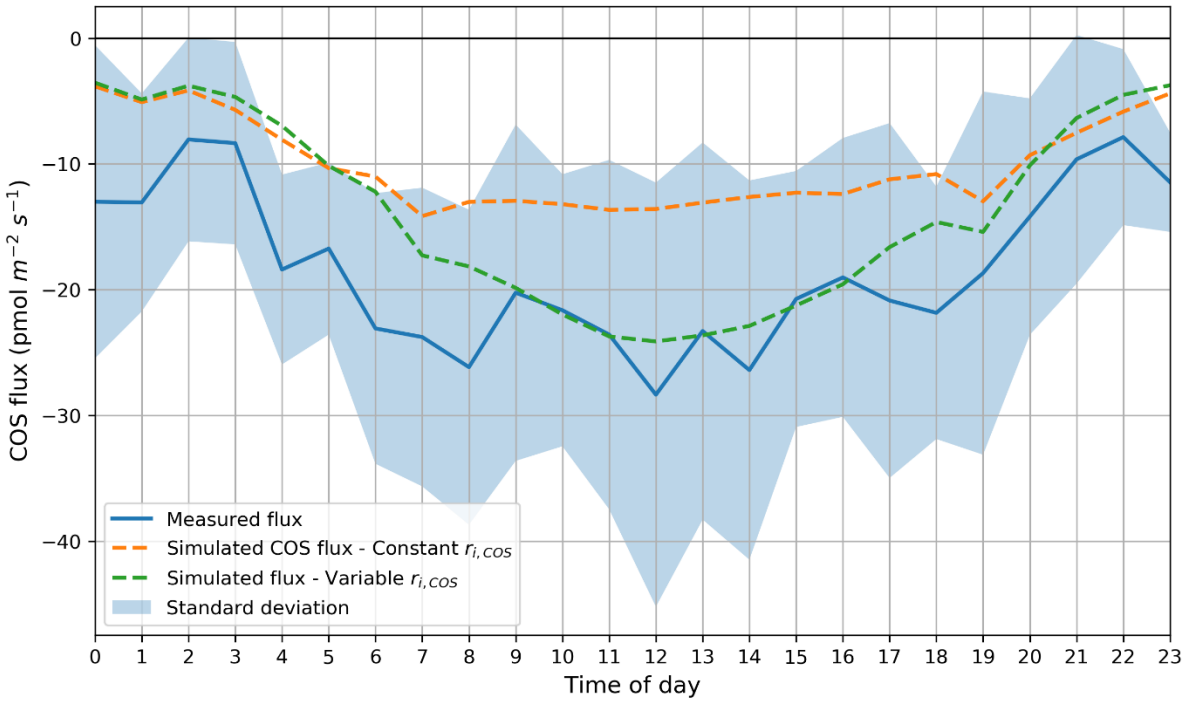

Figure 16: Measured (blue line) and simulated average diurnal COS ecosystem fluxes for July 2015 for simulations with a constant (orange line) and variable (green line) COS internal conductance ($r_{i,COS}$).

3.2.4 Wet vegetation surfaces

The possible influence of uptake of COS by wet vegetation surfaces was already shortly discussed in a previous section. Here we will show a more detailed analysis on the importance of wet vegetation surfaces on COS mixing ratios and fluxes. Little research has been done on this subject, however, even for relatively low solubility, there potentially might be a role of uptake by leaf/needle wetness especially for strongly suppressed turbulent mixing conditions and a large wet surface area (Campbell et al., 2017).

Here it will be shown if it is important to consider the role of COS removal by wet vegetation. This is done using the COS and CO_2 data, but also O_3 is used as it is known that there appears to be enhancement in removal for wet conditions (Altimir et al., 2006). In section 3.2.1 it was shown that COS and O_3 show very comparable diurnal cycles. The similarity in the two tracer's mixing ratio is also shown in Figure 17 where a correlation between O_3 and COS mixing ratios is plotted with a distinction between high and low wet skin fraction (f_{ws}). A relative strong correlation between the two is found, especially for a high f_{ws} with Pearson correlation of 0.667 while for low f_{ws} r=0.230. The relative strong correlation between the COS and O_3 mixing ratios for the wet surface conditions indicates that there might be a similar role of uptake by wet vegetation for these tracers but it could also be that other processes might explain this inferred correlations between O_3 and COS, e.g., limited nocturnal mixing conditions enhancing vegetation wetness as well as the depletion of both compounds.

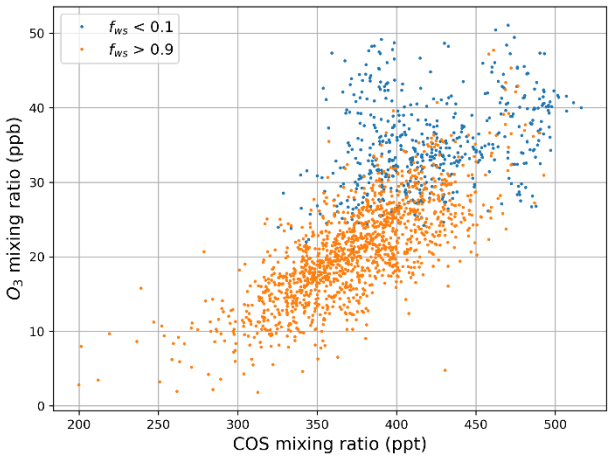

Figure 17: Correlation between measured O_3 and COS mixing ratios plotted for high (orange dots) and low (blue dots) wet skin fraction (f_{ws}) for the entire measurement campaign.

To observe whether the different tracer mixing ratios are indeed influenced by the vegetation wetness we look at the correlation between the tracer and the wet skin fraction. The correlations are shown in Figure 18 and Table 3 for measured COS, O_3 and CO_2 mixing ratios at 4 meters as well as for measured COS and CO_2 deposition velocities using data from June and October 2015. For the correlations regarding deposition velocities and vegetation wetness, only daytime data was used since it is expected that nocturnal deposition velocities will be very small. Further a distinction between July and October was made to prevent scatter caused by seasonality. Correlation between COS mixing ratio and f_{ws} are different for July and October. In July a relatively strong negative correlation can be found while in October no significant trend can be observed. CO_2 mixing ratios show a different trend with high mixing ratios under conditions with high f_{ws}. Both for July and October this trend can be observed, with a slightly steeper slope in July, but stronger correlations in October. O_3 shows the most pronounced trend with a strong negative correlation between O_3 mixing ratios and f_{ws} both in July and October. Less data is available to establish potential dependencies of deposition velocities on the wet skin fraction since only day-time data was used. However, some clear relationships between $V_{d,CO2}$ and f_{ws} can be seen where a distinct negative correlation indicates less deposition (and thus likely smaller fluxes) under more humid conditions. This is the case for both July and October although $V_{d,CO2}$ is already relatively low in October anyway. For $V_{d,COS}$ the trends are less clear and not as significant as for CO_2. For July no significant trend is found with very weak correlation and no clear change in mixing ratios, while October appears to show a slight negative trend with a relatively weak but significant correlation.

Clear differences can be seen in the COS and CO_2 mixing ratios for different f_{ws}. Where the CO_2 mixing ratios increase with increasing f_{ws} the COS mixing ratios tend to decrease or stay more or less the same. The $V_{d,CO2}$ shows a clear decreasing trend with increasing f_{ws} of a factor 2 to 3 when leaves are completely covered with water, while here the COS deposition velocity stays more or less stable but shows less correlation and lower to no significance. The O_3 mixing ratios show the most obvious trend and clearly decrease with increasing f_{ws}. Before drawing any conclusions from this we will first analyse diurnal cycles in simulated and measured COS, O_3 and CO_2 mixing ratios under different f_{ws} conditions.

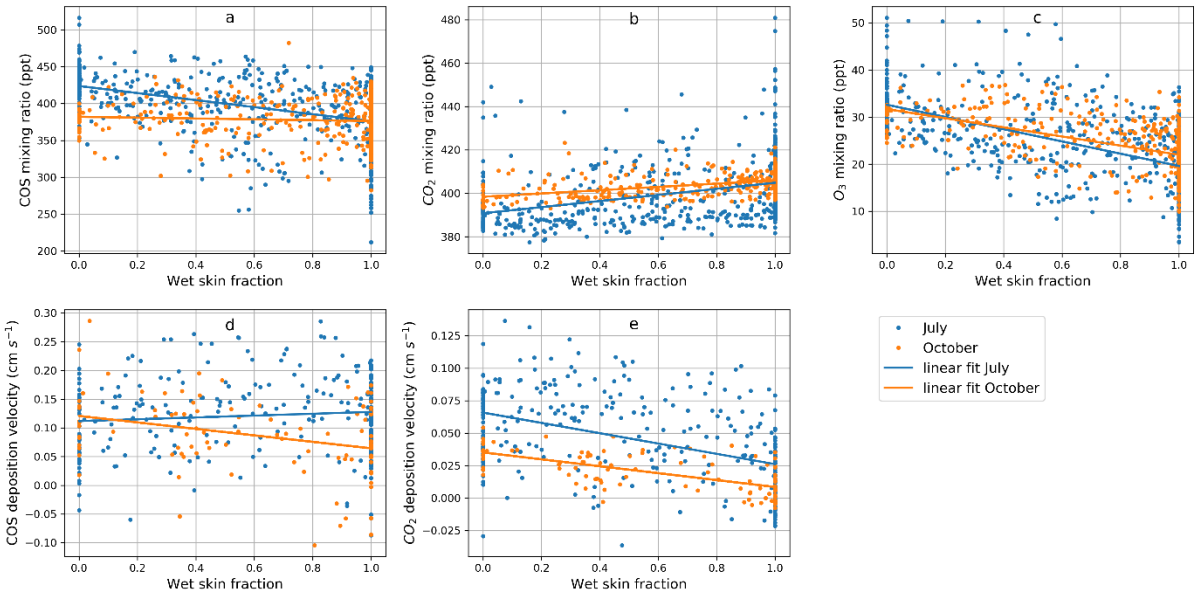

Figure 18: Correlation between the measured a) COS, b) CO_2 and c) O_3 mixing ratio as well as the d) COS and e) CO_2 deposition velocity and simulated wet skin fractions for July (in blue) and October (in orange) 2015 (correlations and significance are given in Table 2).

Table 3: Pearson correlations between tracer mixing ratios and deposition velocities with f_{ws} and its significance for July and October 2015.

	July		October	
	Correlation with f_{ws} (pearson r)	Significance (p-value)	Correlation with f_{ws} (pearson r)	Significance (p-value)
COS mixing ratio	-0.434	<< 0.01	-0.063	0.183
CO_2 mixing ratio	0.363	<< 0.01	0.459	<< 0.01
O_3 mixing ratio	-0.598	<< 0.01	-0.592	<< 0.01
COS deposition velocity	0.093	0.128	-0.317	0.001
CO_2 deposition velocity	-0.470	<< 0.01	-0.657	<< 0.01

It is expected that uptake by wet vegetation has the largest impact on night-time mixing ratio due to stable conditions. Little mixing will deplete COS within the canopy as little air from above the canopy will replenish the in-canopy mixing ratios as it is taken up by the soil. The night-time is often also the time with the largest area covered with water due to dew formation on the leaves (Klemm et al., 2002). However, for GPP calculations the night-time COS fluxes are not important due to a zero night-time GPP, but it could provide us with insight in what processes occur during more humid days. In addition, the reduction in night-time in-canopy COS mixing ratio may also affect the early morning COS fluxes as mixing ratio gradients between the air and the leaf decrease. Figure 19 shows the average diurnal cycle in simulated COS mixing ratio at 4 and 12 meters under high (>0.9) and low (<0.1) f_{ws} for two simulations with different water uptake resistances (r_{ws} = 10^4 and 10^5 s m^{-1}) for the month of August. Both an r_{ws} of 10^4 and 10^5 can be considered to reflect only a small efficiency of uptake by vegetation wetness, but despite this a clear difference in COS mixing ratios can be observed between the two simulations. When a high f_{ws} is present COS mixing ratios are lower for the simulation with a lower r_{ws}. During day-time mixing ratios are about 5 ppt smaller when a lower r_{ws} is assumed while at night the difference can be as high as 25 ppt. This shows that, despite a small uptake rate by vegetation wetness, COS mixing ratios can be considerably different than when it is assumed that no uptake by water occurs with the largest impact at night as discussed earlier.

Figure 20 shows the mean measured COS mixing ratios under high and low f_{ws} as well as for CO_2 and O_3 for August 2015. The measured COS mixing ratio at 4 and 14 meters is usually lower with a higher f_{ws}, most clearly at 14 meters height as was seen for the simulated mixing ratios. At a height of 4 meters the soil also has a considerable impact on the COS mixing ratios resulting in a smaller impact of wet vegetation. For O_3 the same is found where the difference in mixing ratio between high and low f_{ws} is very large indicating that under humid conditions the O_3 is decomposed or efficiently removed by vegetation wetness. CO_2 on the other hand usually has higher mixing ratios under high f_{ws}, opposite to the other tracers. When comparing the simulated and measured COS mixing ratios under the different f_{ws} it appears that the simulations with an r_{ws} of 10^4 compares slightly better with the measurements than the extremely high r_{ws} of 10^5. Mainly when looking at simulated COS mixing ratios at 12 meters during the night. Where the simulation with an r_{ws} of 10^5 gives night-time simulated mixing ratios with a high f_{ws} close to the values found when having a low f_{ws} (and sometimes even higher mixing ratios), the r_{ws} of 10^4 has much lower night-time mixing ratios in a comparable way as the measurements. The same can be found when we compare the measured COS ecosystem fluxes with the two simulations as is shown in Figure 21. Simulated ecosystem fluxes for the simulation with a r_{ws} of 10^4 are much closer to the measured ecosystem flux than for the simulation with an r_{ws} of 10^5 for both the night and during the day. However, differences in the measured and simulated diurnal cycles and strong variability in COS

mixing ratios over a day makes it difficult to analyse these results. Besides, it was previously found that a different sink could be present at night (incomplete stomatal closure) and that the model might contain a misrepresentation of turbulent mixing under stable conditions resulting in other sources of discrepancies between the simulations and the measurements.

It is clear that O_3 has a stronger difference in mixing ratio under different f_{ws} and CO_2 shows different mixing ratios and ecosystem fluxes than COS and O_3. This could suggest that different processes take place for COS and CO_2 during humid conditions which could also explain the differences found in Figure 18. This process could be the uptake of COS by wet vegetation, but this is hard to conclude from this data due to variability in other micrometeorological parameters. The simulations do show a potential for COS uptake by wet vegetation (Figure 19) even with a relatively high wet skin uptake resistance but cannot provide a clear indication on whether this process actually occurs.

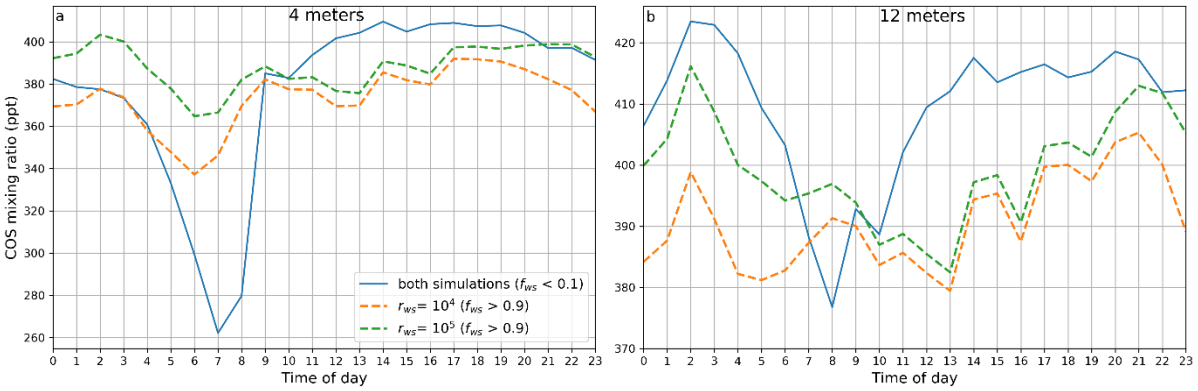

Figure 19: Average diurnal cycles in simulated COS mixing ratio with an r_{ws} of 10^5 (green dotted line) and 10^4 (orange dotted line) at a) 4 meters and b) 12 meters showing mixing ratios under high (>0.9 – dotted lines) and low (<0.1 – blue line) f_{ws} for August 2015. Both simulations show the same mixing ratios under low f_{ws} therefore only one line is shown.

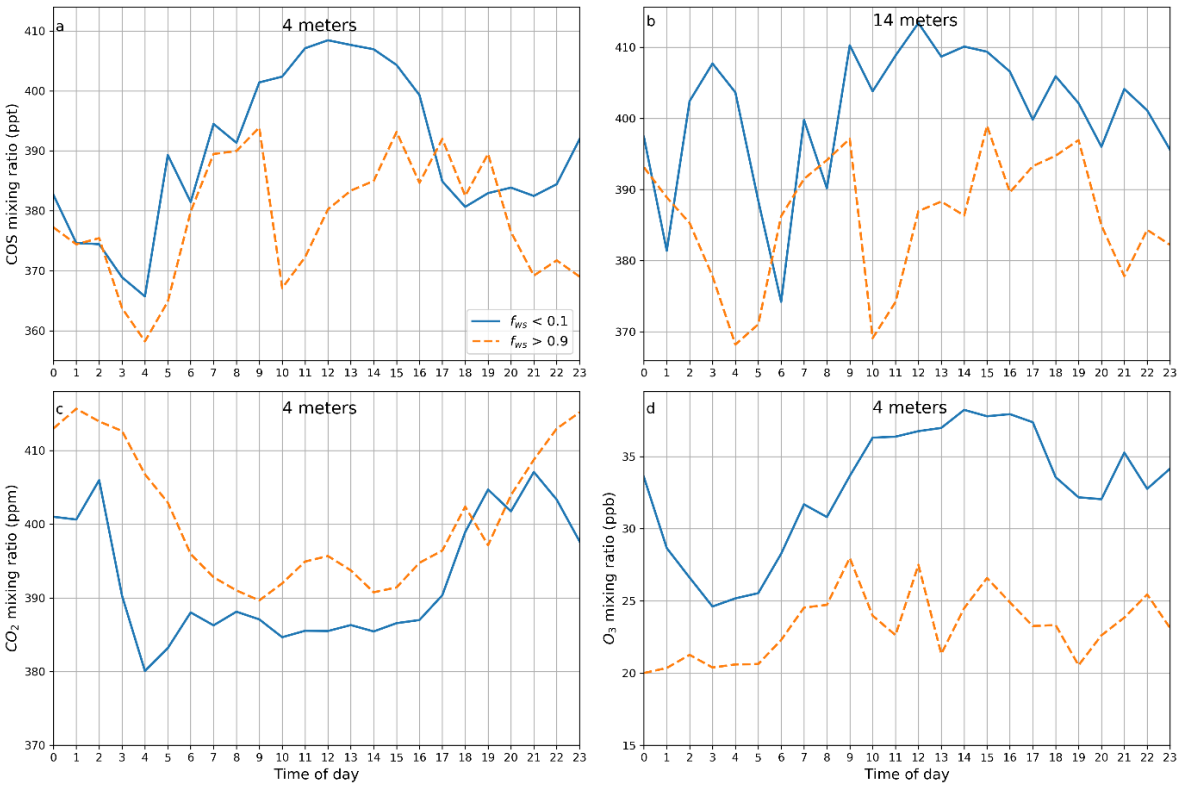

Figure 20: Average diurnal cycles in measured a) COS mixing ratios at 4 meters, b) COS mixing ratios at 14 meters, c) CO_2 mixing ratios at 4 meters and d) O_3 mixing ratios at 4 meters under high (>0.9 –orange dotted line) and low (<0.1 – blue line) f_{ws} for August 2015.

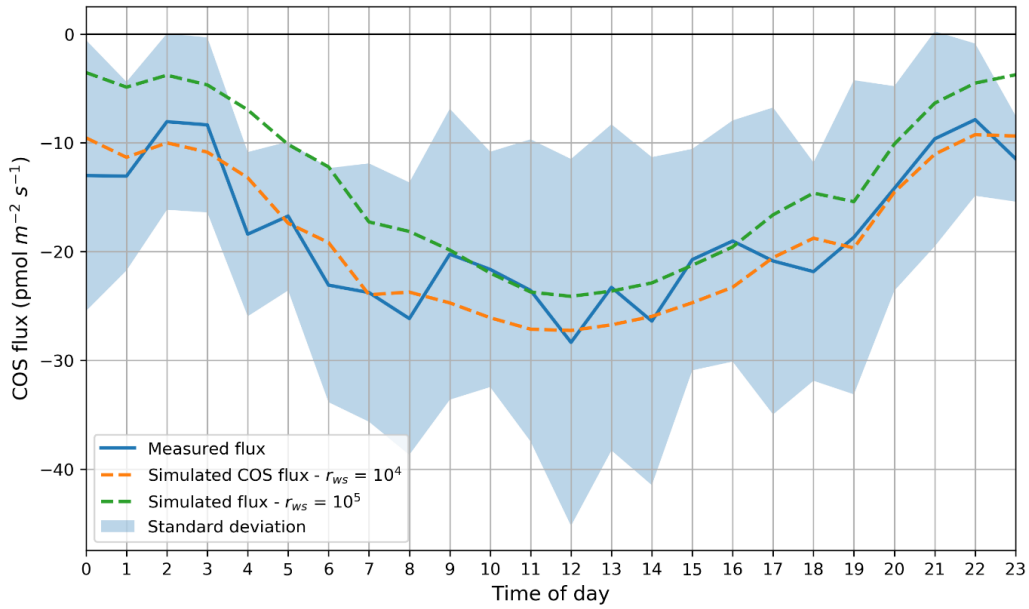

Figure 21: Measured (blue line) and simulated average diurnal COS ecosystem fluxes for July 2015 for simulations with an r_{ws} of 10^4 (orange line) and 10^5 (green line).

3.3 GPP and LRU estimates

GPP was inferred from the measurements and the simulations using both the traditional NEE as well as the COS method. For the COS method both a light dependent LRU as well as a constant LRU, calculated from the simulated and measured fluxes, were used for inferring GPP. This comes down to six different GPP estimates (2 from the NEE method and 4 from the COS method). For making a comparison it is here assumed that the GPP inferred using the traditional NEE method from the measured fluxes provides the best representation of actual canopy CO_2 uptake and therefore this GPP estimate is used as a reference. Also, the LRU inferred from the measurements and simulations will be discussed to provide more insight into the differences between the measured and simulated situations. Figure 22 shows the average diurnal measured and simulated GPP estimates using the traditional NEE method for July and August 2015. The inferred GPP from the simulations show a relatively comparable diurnal cycle up to about 2PM. Thereafter the simulated GPP remains too high compared to the measurements. This diurnal cycle differences in GPP resembles the differences in diurnal cycles in simulated and observed ecosystem fluxes and was possibly caused by differences in the actual on site and simulated VPD effect in the afternoon.

Figure 23a shows the mean diurnal LRU inferred from the simulated and measured data for the months July and August. The two show a different diurnal cycle and are only the same around the middle of the day. The LRU is calculated as the ratio between $F_{e,COS}$ and $F_{e,CO2}$ normalized for their mixing ratios. Therefore, it can here be inferred that the simulated and measured ratio between these fluxes is considerably different in the early morning and afternoon as was already previously shown. The simulated LRU shows a small increase during the day with

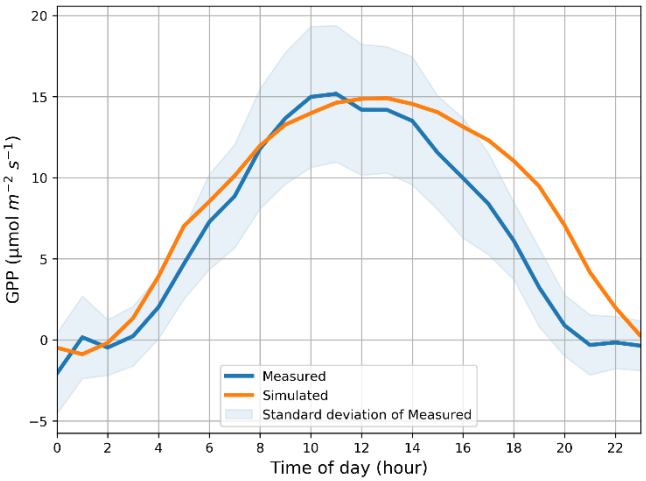

Figure 22: Average diurnal measured (blue line) and simulated (orange line) GPP inferred using the traditional NEE method for the months July and August 2015.

a maximum around noon whereas the measurement inferred LRU shows a continuous decrease in the morning reaching a minimum around noon followed by a steadily increase. Previously it was already seen that the COS and CO_2 mixing ratios as well as ecosystem fluxes are not always simulated correctly with the largest discrepancies between the measured and simulated situation in the early morning and late afternoon. It was therefore expected that at these times simulated LRU are quite different compared to the measured LRU. This difference in diurnal cycle for LRU also results in a different relation between simulated and measurement inferred LRU and photosynthetic active radiation (PAR) as can be seen in Figure 23b. In addition, also the PAR dependent LRU (LRU = 607.26/PAR + 0.57) derived by Kooijmans et al., 2019 using the same measurement data as in this study is shown. Obviously, the measurement inferred LRU therefore corresponds well with the PAR dependent LRU. Simulated LRU does however not appear to show any significant correlation with PAR although a slight decrease in LRU occurs with very low PAR. The PAR dependent LRU shown in Figure 23 is used to calculate GPP for both the measured and simulated data as well as a constant LRU obtained from the median measured and simulated LRU. The median is used here as the measured LRU values have a relatively high density around lower values with some very high outliers at low radiation (at which times GPP will be lower too). Simulated median LRU is 1.1 while the median of the measured LRU is 1.6 a value reported by multiple previous studies (Billesbach et al., 2014; Stimler et al., 2012).

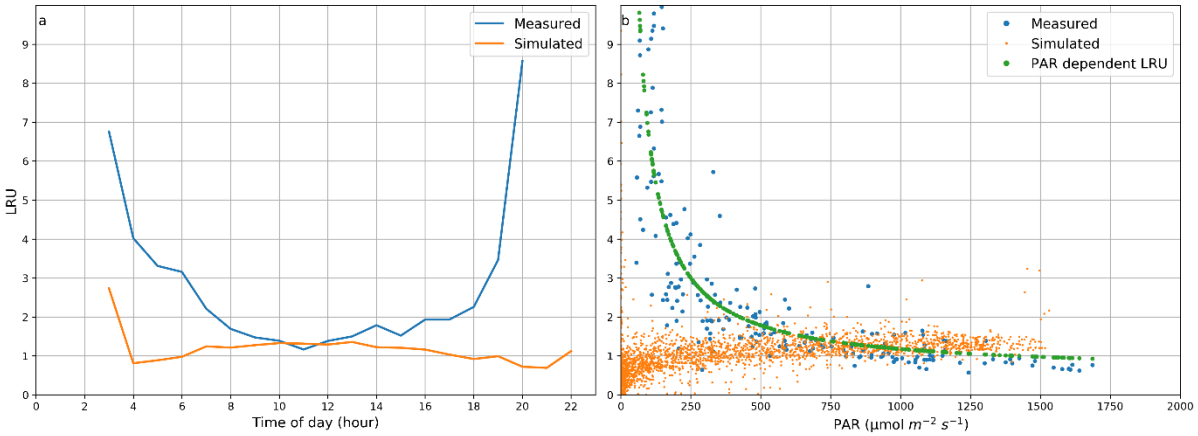

Figure 23: a) Average diurnal cycle in measured (blue line) and simulated (orange line) LRU for the months of July and August 2015, b) Photosynthetic active radiation (PAR) plotted against day-time LRU for measured (July & August 2017 - blue dots), simulated (July & August 2015 - orange dots) and a PAR dependent LRU (LRU = *607.26/PAR + 0.57,* Kooijmans et al., 2019) *(based on July and August 2017 measured data – green dots).*

Resulting GPP inferred using these LRU values are shown in Figure 24 where they are compared to the GPP inferred from the measurements using the NEE method. Measured COS based GPP estimates show a larger variability over a day than with the CO_2 method, which shows a relatively smooth diurnal cycle. Both the GPP from the PAR dependent LRU as well as the estimate with a constant LRU show the diurnal variations. However, measurement inferred GPP from the PAR dependent LRU is much closer to the GPP estimates from the CO_2 method as it shows higher peak values around noon as well as lower values at the start and end of the day. The COS method appears to work relatively well for the measurements when using this PAR dependent LRU, where only the daily variability is larger.

Simulated GPP estimates based on the COS method are relatively close to the measured GPP using the NEE method. Both LRU methods show a similar diurnal cycle in GPP, however the estimates with a constant LRU is always higher than the simulation with the PAR dependent LRU. Peak GPP is too high and occurs slightly too late for both simulated GPP estimates and is generally too high when using a constant LRU. Application of the light dependent LRU on the other hand results generally in too low GPP, most clearly in the early morning, indicating the fact that the simulated LRU does not strongly

depend on PAR. The simulated GPP inferred using the constant LRU closely resemble the simulated GPP inferred from the NEE method (Figure 22) although being somewhat larger. The fact that the GPP inferred from the simulation peaks too late and is too high is also consistent with the observed misrepresentation of especially the stomatal exchange in the afternoon potentially due to misrepresentation of moisture limitation.

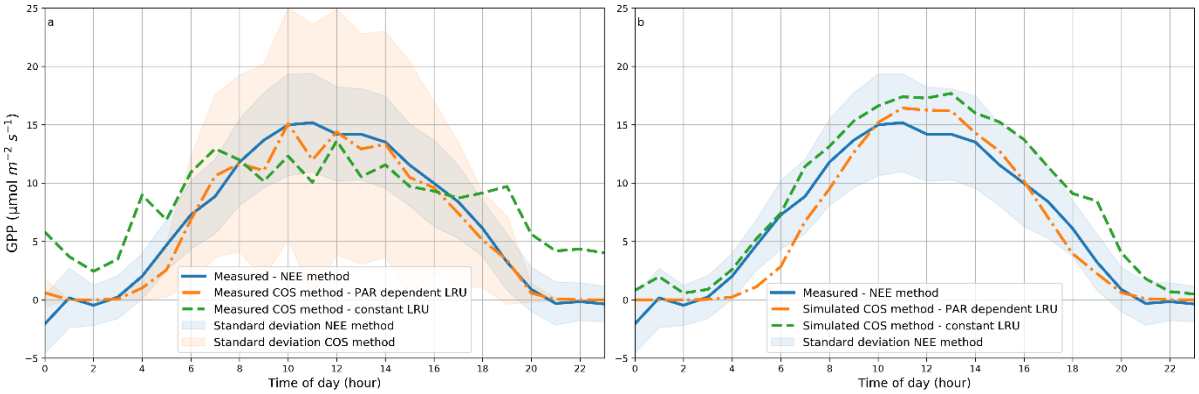

Figure 24: Average diurnal GPP inferred from a) measured and b) simulated fluxes. Both measured and simulated plots compare the measured GPP from the NEE method (solid blue line) with COS method using a PAR dependent LRU (orange dash-dot line) and using a constant LRU (green dashed line) for the months of July and August 2015. The shaded area shows the standard deviation of the measurement inferred GPP.

Both the average measured GPP using the traditional NEE method as well as with the COS method (using the PAR dependent LRU) has a maximum GPP of around 15 μmol m^{-2} s^{-1}. These two approaches to infer GPP also results in comparable average daily GPP estimates of 0.57 and 0.53 mol CO_2 m^{-2} d^{-1}, respectively while when using a constant LRU, the measurements arrive at a lower peak GPP (of around 14 μmol m^{-2} s^{-1}) but a higher daily average GPP of 0.70 mol CO_2 m^{-2} d^{-1} (including the night-time fluxes). The GPP inferred from simulations with the NEE method also arrives at a peak GPP of about 15 μmol m^{-2} s^{-1} but shows considerably higher daily average GPP (0.72 mol CO_2 m^{-2} d^{-1}). The simulated GPP estimate based on the PAR dependent LRU has a peak GPP of 16.4 μmol m^{-2} s^{-1} while the simulations with a constant LRU has a peak of 17.7 μmol m^{-2} s^{-1}, while average daily simulated GPP for these are respectively 0.53 and 0.75 mol CO_2 m^{-2} d^{-1}. When comparing the two simulated COS based GPP estimates with the simulated GPP based on the NEE method it appears that the simulation with a constant LRU corresponds better, however showing a higher peak GPP.

Assuming that the measured GPP using the NEE method gives accurate results it appears that the COS method works relatively well for the measured data when using a PAR dependent LRU. Further, the simulated GPP with a PAR dependent LRU also results in a reasonable GPP estimate compared to the measured GPP, however here it has to be noted that the simulated LRU correlate poorly with PAR. Therefore, it is quite surprising that the PAR dependent LRU actually result in a reasonably accurate simulated GPP estimates. This might indicate that, though this GPP estimate appears accurate, this may be due to the wrong reasons also since the simulated COS flux is underestimated at low light conditions (see section 3.1.2).

4 Discussion

In this section we will reflect on the results and describe the uncertainties and limitations of the measurements and simulations. First the results will be further interpreted by assessing mechanisms taking place within the canopy found during this study as well as relate this to previous research. Next the uncertainties and limitations within the measurements and the model will be discussed. Finally, we will provide a suggestion for future research.

4.1 Processes behind the ecosystem fluxes.

4.1.1 Turbulence and mixing ratios

During this study a comparison was made between COS and O_3 mixing ratios. This has not seen much attention before, despite the two tracers following similar diurnal cycles. However, during this study a comparison with O_3 could support the study of the diurnal cycle in COS mixing ratios. It was not possible to directly assess the relation between the mixed layer growth and changes in COS mixing ratios as no mixed layer depth measurements were available for the measurements period at Hyytiälä. However, the comparison with O_3 supports the observations that it is indeed entrainment that results in the strong increase in the early morning COS mixing ratios (Hastie et al., 1993). This is supported by Montzka et al., 2007, who showed that the COS mixing ratios in the free atmosphere are considerably higher than in the mixed layer (sometimes up to 100 ppt larger (20%)). When turbulent mixing in the early morning increases and the inversion breaks up, COS is entrained from the residual layer above. For CO_2 being emitted by the soil, night-time CO_2 mixing ratios are generally higher inside the canopy and in the surface layer than in the free troposphere resulting in decrease in CO_2 mixing ratio when the mixed layer grows, explaining the different trend compared to COS (Vilà-Guerau de Arellano et al., 2004). The enhanced mixing in the morning within the canopy also result in higher COS mixing ratios while under (night-time) stable conditions mixing ratios tend to decrease potentially leading to depletion within the canopy. This can in particular be of influence on the COS mixing ratios within the leaf boundary layer where mixing ratios could become low as diffusion to this leaf boundary layer decreases with lower in canopy COS mixing ratios, potentially also reducing uptake rates (Kooijmans et al., 2017). It is therefore important to simulate the turbulent mixing within the canopy and between the canopy and the surface layer well. Despite the fact that we have constrained the MLC-CHEM simulations with the observed friction velocity, it appears from the presented evaluation of in-canopy mixing ratios and fluxes that there are still deficiencies in the model's representation of this process. This resulted in some discrepancies between the simulations and the measurements mostly under stable conditions when simulated COS and CO_2 mixing ratios showed strong outliers compared to the measurements. The effect of low u* on the measurements will be discussed in a following section (Section 4.2)

4.1.2 Soil exchange flux

The soil acts as a sink for the entire measurement campaign and appears to be relatively constant. This makes it relatively easy to correct for this additional sink term when calculating GPP. However, this may not be true for other locations as other studies indicate an influence of soil water content and soil temperature on soil COS uptake (Sun et al., 2015; Yang et al., 2019). Yang et al., 2019, also found that soils that receive sunlight are more prone to COS emissions possibly due to higher temperatures or due to different processes in the soil (e.g. less biotic activity due to further distance to roots). A lot of heterogeneity has been reported in soil fluxes across different biomes with highest reported emission fluxes in senescing agricultural fields of up to 30 pmol m^{-2} s^{-1} (Maseyk et al., 2014) and highest uptake fluxes of around -11 pmol m^{-2} s^{-1} at a riparian forest site (Berkelhammer et al., 2014). It appears that the soil is more likely to become a source for COS under high temperatures (>20 °C) (Maseyk et al., 2014; Whelan et al., 2018; Yang et al., 2019). However, at Hyytiälä these temperatures do not occur frequently possibly explaining the apparent rather constant uptake of COS by the soil. The measured soil COS fluxes were for a large part performed with a soil temperature between 10 to 16 °C. This small range of soil temperatures might also be a reason why no significant correlation between soil temperature and COS fluxes are found.

4.1.3 Night-time stomatal uptake and diurnal wet skin uptake

The night-time COS fluxes indicated that besides the soil deposition flux another considerable sink is present at night. As mentioned in the results this can be incomplete stomatal closure or the uptake by wet vegetation. During this study it was not possible to assess their importance due to the large amount of variability in other micrometeorological conditions and a lack of specific measurements. It however is necessary to understand which process causes the difference between the night-time soil and ecosystem fluxes. Where an incomplete nocturnal stomatal closure will only have an effect on night-time fluxes the uptake by wet vegetation surfaces can also influence day-time fluxes and in-canopy mixing ratios. During this study it was found that night-time stomatal conductance usually is non-zero which would explain the relatively high ecosystem flux at night. Previous studies (including those on COS) have suggested the occurrence of night-time incomplete stomatal closure (Commane et al., 2015; Kooijmans et al., 2017). However, these studies did not take into account the potential uptake of COS by wet vegetation surfaces. In addition to that, a study on incomplete stomatal closure found that for coniferous vegetation only little nocturnal stomatal opening takes place (Caird et al., 2007).

Little research has been done on the impact of uptake by wet vegetation. According to a study by Campbell et al. (2017), the uptake of COS by fog water is only minimal compared to vegetation uptake, however they do mention that more research is required on this to be certain. The results found in this study give an indication that uptake of COS by wet vegetation can potentially play a role in explaining observed nocturnal fluxes even if the uptake resistance is relatively high ($r_{ws} = 10^4$ s m^{-1}). Here we also refer to the demonstrated similarities between COS and O_3 as they both show decreasing mixing ratios under higher wet skin fractions. O_3 appears to be taken up and decomposed efficiently by vegetation wetness (Altimir et al., 2006; Gerosa et al., 2009) with a Henry's law constant ($K_H = 1.1*10^{-4}$ mol m^{-3} Pa^{-1}) that is comparable to that of COS ($K_H = 2.0*10^{-4}$ mol m^{-3} Pa^{-1}) and CO_2 ($K_H = 3.4*10^{-4}$ mol m^{-3} Pa^{-1}) (Sander, 2015) which results in observed vegetation O_3 uptake rates much larger than what is expected based on this Henry's law constant. These discrepancies have been attributed to an enhancement in uptake also due to aqueous phase chemical decomposition (Altimir et al., 2006) triggering the question how COS is further involved in aqueous phase processing. Besides the hydrolysis of COS with H_2O, COS has also been found to react with OH when dissolved in natural water possibly resulting in higher decomposition rates for alkaline conditions (Elliott et al., 1989). Further it has been found that the hydrolysis of COS can be a base-catalysed reaction with the strength of the base being an important effect on hydrolysis rates of COS (Zhao et al., 2013). Therefore, despite no strong influence of pH on the dissolution of COS (Elliott et al., 1989) it appears that the decomposition of COS can be affected by pH. CO_2 mixing ratios and deposition velocities show considerable differences with those of COS under humid conditions and therefore different processes appear to occur. It is expected that the CO_2 shows a lower deposition under high f_{ws} conditions potentially due to stomatal blocking by water droplets (Wesely, 1989). Wesely indicates that up to two thirds of the leaves can be covered in water, decreasing uptake by a factor of three, which is close to the magnitude found during this study with 60% lower CO_2 deposition velocities for July under maximum wet skin fraction. COS should have the same pathway into the leaf and therefore is expected to show the same behaviour as CO_2. However, this is not found as deposition velocities change little as a function of changing humidity. This indicates that other processes take over the stomatal uptake of COS when the stomata are blocked by water such as the uptake of COS by canopy wetness. Assuming the water is indeed a significant sink for COS than this could influence the COS flux and therefore the inferred GPP considerably. It must be noted that the hydrolysis of COS in water, the only process known to removes COS from water, is a very slow process at atmospheric temperature and close to neutral pH, compared to the average time the vegetation is covered with water (Whelan et al., 2018). Therefore, it

is expected that a relatively large amount of the COS taken up by water moves back into the atmosphere as the water evaporates resulting in a sharp rise in COS mixing ratios and lower COS uptake fluxes. This is however hard to observe since hourly averaged data is used during this study and this process was therefore not found. Further, it may be that the decomposition of COS in water is enhanced by the presence of carbonic anhydrase in the water. This may come from microorganisms present on the leaf surface (epiphytic microbes) that end up in the water when dew is forming and potentially resulting in enhanced hydrolysis of COS reducing its mixing ratio in the water (Campbell et al., 2017). However, this process has not been observed so far and would require more research (Whelan et al., 2018).

4.2 Limitations and uncertainties

4.2.1 Measurements

Both the simulations and the measurements have some degree of uncertainty while the model showed some additional limitation with respect to simulating COS and CO_2 fluxes. First of all, the soil flux measurements are only measured in the dark, while the processes involved in the respiration and uptake of COS could depend on light and temperature resulting in an uncertainty in the soil flux measurements (Yang et al., 2019). It has been suggested that the soil uptake of COS is mostly depending on carbonic anhydrase in the decomposing leaves and soil and by microbial activity (Sun et al., 2018). Potential influence of sunlight on soil temperatures and microbial activity is thus reduced potentially being the result of the limited difference in measured fluxes between day and night. However, this will likely not influence the night-time fluxes and therefore does not explain the difference between the measured night-time ecosystem and soil flux.

Other uncertainties regarding the measurements arise due the measurement quality of COS mixing ratios. Due to the low atmospheric COS mixing ratio it is harder to measure than CO_2 mixing ratios. Kooijmans et al., 2016 found that COS measurements are not as precise as CO_2 measurements thereby also causing less precise COS ecosystem fluxes. This current limitation in COS measurements is an important reason why we cannot estimate GPP based on COS as precise as using the traditional method. Future advances in measurement technology could reduce this problem making the COS method a more interesting tool for inferring GPP.

Further, it is important to note that at night as well as sometimes during the day the friction velocities are so low that accurate flux measurements are not available. The flux measurements depend on u* since the turbulence will bring the in-canopy air up to the measurement point as well as that the eddy covariance measurements itself depends on turbulent air (Aubinet et al., 2012; Barr et al., 2013). A minimum value of 0.25 m s^{-1} was used as lower threshold for the shear velocity following the findings of Barr et al. (2013) from comparable coniferous forests. This, however, does result in a less flux data for periods with stable conditions. These stable conditions can potentially be important though given that stable conditions result in substantially lower in-canopy COS mixing ratios as it is taken up by the vegetation and soil. When these conditions last a considerable amount of time this could result in depletion of COS within the canopy, eventually leading to lower fluxes (Kooijmans et al., 2017). This shows that the (nocturnal) flux measurements might be biased towards higher fluxes. The use of deposition velocities is therefore required to remove the influence of changes in COS mixing ratios on COS uptake.

4.2.2 Model

MLC-CHEM has some limitations when it comes to simulating the COS flux also based on some of the essential assumptions on still rather unconstrained processes. First, the calculation of the wet vegetation fraction is based on a simple empirical relation. However, in reality this is likely to be more complex

due to differences in plant physiology and seasonal and micrometeorological variability (Klemm et al., 2002). But no measurements were available regarding vegetation wetness therefore these results should be viewed with caution (Yanez-Serrano et al., 2018). The model appears to overestimate the vegetation wetness fraction estimated from the observed relative humidity as a large amount of the data show very high f_{ws} values shown in Figure 25. The frequency distribution of f_{ws} values is plotted in bins of a fraction of 0.02 for the entire simulated period (June until October). Since most of the data show a high or complete cover of vegetation with water it may overestimate the uptake of soluble substances considerably. However, this is again hard to analyse due to the lack of measurements on the wet skin fraction. Besides this, the model also contains no saturation point to tracer mixing ratios in water and once the tracer is taken up by the water it disappears from the system. As a result, during extensive periods of high wet skin fraction, it is likely that the actual tracer uptake would be in equilibrium with its chemical decomposition. Instead the model keeps taking up the tracer indefinitely creating a potential for large tracer uptake as well as no release of tracers when the water evaporates. Due to these limitations and the lack of measurements on wet vegetation fraction it is hard to draw any conclusions of the effect on COS uptake. The role of wet vegetation as well as the potential of the decomposition of COS in the water should be studied in more detailed in a controlled environment. A potential for a considerable wet vegetation sink is present but would likely require the decomposition of COS in the water or COS should be re-emitted into the atmosphere as the vegetation water evaporates. These processes could not be observed during this study but could potentially influence COS mixing ratios and ecosystem fluxes and should therefore be studied in more detail.

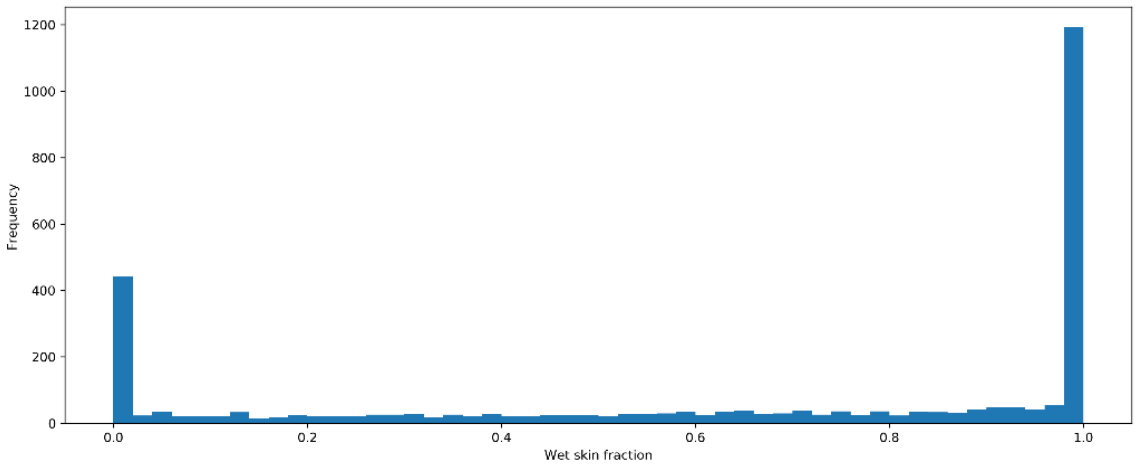

Figure 25: Frequency of simulated wet skin fractions during the entire measurement campaign using bins of 0.02.

Nocturnal stomatal conductance was set to zero for the final default settings. This was partly due to the fact that no clear evidence was found for the presence and magnitude of incomplete stomatal closure. However, if nocturnal stomatal opening does take place and would be incorporated into the model this would have resulted in incorrect night-time CO_2 fluxes. This is due to the fact that MLC-CHEM does not take the light requirement of the CO_2 reaction by Rubisco into account and therefore keeps taking up CO_2 even when it is dark. This would have resulted in lower night-time CO_2 mixing ratios and possibly also impacted the LRU calculations. Measurement inferred LRU is found to be light dependent due to the fact that the COS uptake is independent of light while that of CO_2 is dependent of light (Kooijmans et al., 2019). Therefore, if the ratio in uptake velocities between the two tracers is calculated a light dependent relation is found. The fact that this light dependence of CO_2 is missing in MLC-CHEM possibly combined with the missing night-time stomatal opening causes the incorrect LRU from the simulations.

Besides the limitations to the simulated stomatal conductance the internal conductance is also not simulated entirely correct. The simulated COS ecosystem fluxes are found to be most comparable to the observed COS fluxes using a variable COS internal resistance with a diurnal cycle comparable to the stomatal conductance (but of different magnitude) compared to a constant internal resistance. This could indicate that the diurnal cycles in internal resistance for COS is comparable to the stomatal resistance. However, the measurements do indicate that the measured COS internal conductance has a somewhat different diurnal cycle than the stomatal conductance. This can indicate that though the model gives correct fluxes it might be for the wrong reasons also recognising that the simulated diurnal cycle in stomatal conductance might be different compared to the diurnal cycle in the actual site g_s. The current implementation of $r_{i,COS}$ is a simplification that could result in incorrect diurnal cycles of this parameter. Currently not enough is known about the internal resistance of COS and therefore it was not possible to implement this properly in the model (Wohlfahrt et al., 2012) potentially being another reason as to why the simulated LRU is not as strongly related to PAR like the measurements shows. Furthermore, no measurements of stomatal conductance were available for the simulated period and therefore the simulated stomatal conductance could not be verified. The simulated vegetation conductance (sum of all leaf conductances) in A-g_s may result in a simulation of CO_2 fluxes that generally agree well with the observations, however this could still reflect a misrepresentation of the contribution by stomatal and internal conductance. Therefore, despite a good representation of the CO_2 flux it will result in a misrepresentation of COS uptake since the internal conductance term is different than for CO_2. This difference between the internal COS and CO_2 conductance arise due to their difference in enzymatic reaction (Carbonic anhydrase and Rubisco respectively), where carbonic anhydrase (CA) is assumed to catalyse the reaction of COS very efficiently resulting in lower mesophyll COS concentrations (Seibt et al., 2010). This high efficiency of CA suggests that the internal conductance for COS should be less limiting than the stomatal conductance, however it was found that this is not the case, indicating that the COS diffusion to the reaction site is likely an important factor for internal COS conductance (Seibt et al., 2010).

Other reasons for errors in the simulated COS and CO_2 fluxes arise due to potential errors in LAI and the leaf area density (LAD). Although a representative average value has been used for LAI, given that Hyytiälä's forest is somewhat heterogeneous (Heiskanen et al., 2012), the amount of biomass involved in COS and CO2 uptake might be different for different footprints. In addition, we also applied this average LAI in the simulation for the whole measurement campaign assuming no change during a growing season. The same goes for the LAD, in the model it is assumed that there is a uniform profile indicating no differences in leaf density between the understory and the crown layer. This is likely not accurate and a simplification of reality as the largest part of the canopy is found above 7 meters (Kooijmans et al., 2017). The LAD profile is an important feature given that it has multiple effects including e.g. the distribution of the sun versus shaded leaf area but also determines the in-canopy turbulent mixing intensity.

Finally, there is some inaccuracies in the model due to measurement errors and quality. Since the simulated meteorological and above-canopy tracer mixing ratios were constrained by the measurements the quality of the simulations depends on the quality of these measurements. Mostly the COS mixing ratios imposed on the model by the measurements appear to show some issues with their quality. When investigating the timeseries of the measured mixing ratios in more detail large hourly differences are found, where a more smoothed hourly pattern is expected like the mixing ratios of CO_2. This variability in the measured COS mixing ratios likely occurs due to the less precise measurements of this tracer and is therefore expected to be not representative for the actual conditions and could result in incorrect fluxes as well (Kooijmans et al., 2016). However, what can be seen is that the concentrations in the

canopy (which are inferred by the model) have a lower variability in mixing ratios and also the simulated COS fluxes show a much smaller hourly variation than the measurements. This indicates that the model reduces the hourly variability in the measurements, but this may still lead to a somewhat incorrect mixing ratios. It is therefore suggested that for future studies with this kind of data the variability is reduced by applying some kind of smoothing (e.g. using 3-hour average).

4.3 Future research

From this study it becomes apparent that more research is required on in-canopy COS processes to be able to simulate in-canopy mixing ratios and canopy top fluxes accurately. This could include a more in-depth comparison of COS and O_3 using besides the mixing ratios also flux measurements which were not available for this research period. A study of night-time COS fluxes should be performed to better understand the processes taking place at night besides the soil fluxes. Studying the night-time COS processes could also provide better insights in processes taking place during the day. Further the COS uptake by wet vegetation surfaces should see more research as during this thesis it was found that wet vegetation surfaces potentially take up considerable amounts of COS, however, it was not possible to study this in detail due to missing measurement data on wet skin fraction and due to variation in other micrometeorological conditions. It is therefore proposed to study the impact of COS uptake by wet vegetation surfaces in a controlled environment to keep other conditions the same. Finally, a better understanding of the internal conductance of COS is required in order to simulate canopy exchange fluxes with a canopy exchange model. The LRU appears to be strongly related to PAR, a feature not reproduced in the simulations to some extend due to a misrepresentation of the internal conductance for COS (besides the missing CO_2 light dependence in the model). Future research into GPP inferred from COS should also consider comparing these results to other methods besides the traditional NEE method as multiple other promising methods for inferring GPP are being developed (e.g. with use of remote sensing and sun-induced chlorophyll fluorescence). Other methods also have their strengths and weaknesses, so it has to be studied whether the COS based method has an added value and what this added value is.

5 Conclusion

In this study a multi-layer canopy scale model was used to better understand the in- and above-canopy processes influencing the in-canopy COS mixing ratios and COS ecosystem fluxes. Simulated COS, CO_2 and O_3 data was compared with measurements at the boreal forest site at Hyytiälä. This study shows that the model simulates the COS and CO_2 in-canopy mixing ratios and ecosystem fluxes reasonably well, but that there are substantial discrepancies regarding the timing in the diurnal cycle. For example, peak fluxes are often simulated well regarding the magnitude but there are considerable large differences between simulated and observed COS and CO_2 mixing ratios and fluxes for the early morning and late afternoon.

To improve the model in- and above-canopy processes were studied. Here it was found that at night the soil is a major sink responsible for around 40% of the total ecosystem flux while during the day the soil is less significant (up to 20%). However, the evaluation indicates that one or more night-time COS sinks, besides the soil uptake, controls the ecosystem COS fluxes. This additional sink could be incomplete stomatal closure and/or uptake by wet vegetation surfaces. Measurements of night-time stomatal conductance do give indications about the presence of incomplete stomatal closure, but since there is only data for June, this result may be caused by the short night with only a few hours with no radiation, which cannot be deemed representative for the entire period of the campaign. However, for GPP calculations based on the COS uptake approach this term is not important since there is no

productivity at night. Uptake by wet vegetation surfaces can be important during the day, and therefore it is important to improve our understanding of the role of canopy wetness in COS uptake. It appears that COS mixing ratios as well as deposition velocity respond differently to increasing wet skin fraction compared to CO_2, possibly indicating that different processes are taking place. Where CO_2 deposition velocities decrease under wet conditions, for COS the removal rates do not change. However, variability in other micrometeorological processes (also influencing mixing ratios and fluxes) make it hard to observe the true impact of wet vegetation since we cannot see the potential effect of the wet vegetation independent of these other micrometeorological parameters. The simulations do provide us with an idea of the potential effect of wet vegetation uptake using two simulations with a different wet skin uptake resistance (10^4 and 10^5 s m^{-1}). Despite both representing a relatively low efficiency in COS uptake, a considerable difference in simulated COS mixing ratios is found of up to 25 ppt during the night and early morning. Further, the measured ecosystem fluxes appear to compare better with simulated ecosystem fluxes using the lower wet skin uptake resistance (10^4 s m^{-1}). This study has shown the potential impact of wet vegetation on the COS mixing ratios and fluxes which would need to be taken into account. However, more research is needed to get a better understanding of this process considering both vegetation wetness measurements but also conducting controlled experiments to study the COS uptake efficiency by leaf water independent of other exchange processes.

An additional term that should be better constrained is the internal conductance of COS as currently it is not possible to accurately simulate this. The internal resistance is on average 2.6 times higher than the stomatal resistance, however the diurnal cycle in $g_{i,COS}$ is not exactly the same as $g_{s,COS}$. Therefore, when scaling the simulated $g_{i,COS}$ with the $g_{s,COS}$ this results in an incorrect diurnal cycle which will also have an influence on the LRU and GPP calculations.

Finally, the simulated and measured GPP was inferred using the traditional NEE method as well as with the COS method using both a constant as well as a PAR dependent LRU. When assuming that the measured GPP using the NEE method is accurate it appears that the measured GPP using the COS method and a PAR dependent LRU infers the GPP well. The model on the other hand shows a different relation between LRU and PAR due to the different diurnal trends in the simulated data compared to the measurements. However, despite this different relation with PAR, resulting GPP using both the constant as well as the PAR dependent LRU agreed relatively well with the measured GPP. It is however possible that this simulated GPP agrees well with the observation inferred GPP for the wrong reasons given the identified issues on simulated COS ecosystem fluxes and mixing ratios.

Using COS to infer GPP is not a very easy task, mainly since many processes need to be considered. It is here, and in previous studies, shown that it is possible to calculate GPP reasonably well, but for now it is no more accurate than using the traditional NEE method. More research will be required to improve our understanding of the processes to reduce the uncertainty in COS fluxes as well as improved measurement techniques are desirable in order to measure COS mixing ratios and fluxes more precise. To improve our modelling capabilities (using canopy scale models) of COS fluxes and mixing ratios it is required to improve our understanding of the internal resistances, impact of uptake by wet vegetation and the mechanisms that explain variability in soil fluxes. Finally, a comparison with other methods available to calculate GPP (e.g. with use of remote sensing) is required to assess which method is most accurate and whether the use of COS has any added value given the current uncertainty in COS measurements.

References

Altimir, N., Kolari, P., Tuovinen, J., & Vesala, T. (2006). Foliage surface ozone deposition: a role for surface moisture? *Biogeosciences*, *3*, 209–228.

Aneja, V. P., Arya, S. P., Li, Y., Murray, G. C., & Manuszak, T. L. (2000). Climatology of diurnal trends and vertical distribution of ozone in the atmospheric boundary layer in urban north carolina. *Journal of the Air and Waste Management Association*, *50*(1), 54–64. https://doi.org/10.1080/10473289.2000.10463984

Asaf, D., Rotenberg, E., Tatarinov, F., Dicken, U., Montzka, S. A., & Yakir, D. (2013). Ecosystem photosynthesis inferred from measurements of carbonyl sulphide flux. *Nature Geoscience*, *6*(3), 186–190. https://doi.org/10.1038/ngeo1730

Aubinet, M., Vesala, T., & Papale, D. (2012). Eddy Covariance: A Practical Guide to Measurement and Data Analysis. In *Springer Atmospheric Sciences Series* (Vol. 12, p. 438). https://doi.org/10.1007/978-94-007-2351-1

Barr, A. G., Richardson, A. D., Hollinger, D. Y., Papale, D., Arain, M. A., Black, T. A., … Schaeffer, K. (2013). Use of change-point detection for friction-velocity threshold evaluation in eddy-covariance studies. *Agricultural and Forest Meteorology*, *171–172*, 31–45. https://doi.org/10.1016/j.agrformet.2012.11.023

Berkelhammer, M., Asaf, D., Still, C., Montzka, S., Noone, D., Gupta, M., … Yakir, D. (2014). Constraining surface carbon fluxes using in situ measurements of carbonyl sulfide and carbon dioxide. *Global Biogeochemical Cycles*, *28*(2), 161–179. https://doi.org/10.1002/2013GB004644

Billesbach, D. P., Berry, J. A., Seibt, U., Maseyk, K., Torn, M. S., Fischer, M. L., … Campbell, J. E. (2014). Growing season eddy covariance measurements of carbonyl sulfide and CO2 fluxes: COS and CO2 relationships in Southern Great Plains winter wheat. *Agricultural and Forest Meteorology*, *184*, 48–55. https://doi.org/10.1016/j.agrformet.2013.06.007

Bonan, G. (2016). *Ecological Climatology*. https://doi.org/10.1017/CBO9781107339200

Caird, M. A., Richards, J. H., & Donovan, L. A. (2007). Nighttime Stomatal Conductance and Transpiration in C3 and C4 Plants. *Plant Physiology*, *143*, 4–10. https://doi.org/10.1104/pp.106.092940

Campbell, J. E., Whelan, M. E., Berry, J. A., Hilton, T. W., Zumkehr, A., Stinecipher, J., … Loik, M. E. (2017). Plant Uptake of Atmospheric Carbonyl Sulfide in Coast Redwood Forests. *Journal of Geophysical Research: Biogeosciences*, *122*. https://doi.org/10.1002/2016JG003703

Commane, R., Meredith, L. K., Baker, I. T., Berry, J. A., Munger, J. W., Montzka, S. A., … Wofsy, S. C. (2015). Seasonal fluxes of carbonyl sulfide in a midlatitude forest. *Proceedings of the National Academy of Sciences of the United States of America*, *112*(46), 14162–14167. https://doi.org/10.1073/pnas.1504131112

Elliott, S., Lu, E., & Rowland, F. S. (1989). Rates and Mechanisms for the Hydrolysis of Carbonyl Sulfide in Natural Waters. *Environmental Science & Technology*, *23*(4), 458–461. https://doi.org/10.1021/es00181a011

Ganzeveld, L., Bouwman, L., Stehfest, E., Vuuren, D. P. Van, Eickhout, B., & Lelieveld, J. (2010). Impact of future land use and land cover changes on atmospheric chemistry - climate interactions. *Journal of Geophysical Research*, *115*, D23301. https://doi.org/10.1029/2010JD014041

Ganzeveld, L., Lelieveld, J., Dentener, F. J., Krol, M. C., & Roelofs, G.-J. (2002). Atmosphere-biosphere trace gas exchanges simulated with a single-column model. *Journal of Geophysical Research*, *107*(D16), 1–21.

Ganzeveld, L., Valverde-canossa, J., Moortgat, G. K., & Steinbrecher, R. (2006). Evaluation of peroxide exchanges over a coniferous forest in a single-column chemistry-climate model. *Atmospheric Environment*, *40*, 68–80. https://doi.org/10.1016/j.atmosenv.2006.01.062

Gerosa, G., Finco, A., Mereu, S., Marzuoli, R., & Ballarin-Denti, A. (2009). Interactions among vegetation and ozone, water and nitrogen fluxes in a coastal Mediterranean maquis ecosystem. *Biogeosciences*, *6*(8), 1783–1798. https://doi.org/10.5194/bg-6-1783-2009

Gimeno, T. E., Ogée, J., Royles, J., Gibon, Y., West, J. B., Burlett, R., … Wingate, L. (2017). Bryophyte gas-exchange dynamics along varying hydration status reveal a significant carbonyl sulphide (COS) sink in the dark and COS source in the light. *New Phytologist*, *215*(3), 965–976. https://doi.org/10.1111/nph.14584

Hastie, D. R., Shepson, P. B., Sharma, S., & Schiff, H. I. (1993). The influence of the nocturnal boundary layer on secondary trace species in the atmosphere at Dorset, Ontario. *Atmospheric Environment Part A, General Topics*, *27*(4), 533–541. https://doi.org/10.1016/0960-1686(93)90210-P

Heiskanen, J., Rautiainen, M., Stenberg, P., Mõttus, M., Vesanto, V., Korhonen, L., & Majasalmi, T. (2012). Seasonal variation in MODIS LAI for a boreal forest area in Finland Janne. *Remote Sensing of Environment*, *126*, 104–115. https://doi.org/10.1016/j.rse.2012.08.001

Kaisermann, A., Ogée, J., Sauze, J., Wohl, S., Jones, S. P., Gutierrez, A., & Wingate, L. (2018). Disentangling the rates of carbonyl sulfide (COS) production and consumption and their dependency on soil properties across biomes and land use types. *Atmospheric Chemistry and Physics*, *18*(13), 9425–9440. https://doi.org/10.5194/acp-18-9425-2018

Kesselmeier, J., & Merk, L. (1993). Exchange of carbonyl sulfide (COS) between agricultural plants and the atmosphere: Studies on the deposition of COS to peas, corn and rapeseed. *Biogeochemistry*, *23*(1), 47–59. https://doi.org/10.1007/BF00002922

Klemm, O., Milford, C., Spindler, G., & Putten, E. M. Van. (2002). A climatology of leaf surface wetness. *Theoretical and Applied Climatology*, *71*, 107–117. https://doi.org/10.1007/s704-002-8211-5

Kooijmans, L. M. J., Maseyk, K., Seibt, U., Sun, W., Vesala, T., Mammarella, I., … Chen, H. (2017). Canopy uptake dominates nighttime carbonyl sulfide fluxes in a boreal forest. *Atmospheric Chemistry and Physics*, *17*(18), 11453–11465. https://doi.org/10.5194/acp-17-11453-2017

Kooijmans, L. M. J., Sun, W., Aalto, J., Erkkilä, K. M., Maseyk, K., Seibt, U., … Chen, H. (2019). Influences of light and humidity on carbonyl sulfide-based estimates of photosynthesis. *Proceedings of the National Academy of Sciences of the United States of America*, *116*(7), 2470–2475. https://doi.org/10.1073/pnas.1807600116

Kooijmans, L. M. J., Uitslag, N. A. M., Zahniser, M. S., Nelson, D. D., Montzka, S. A., & Chen, H. (2016). Continuous and high-precision atmospheric concentration measurements of COS, CO2, CO and H2O using a quantum cascade laser spectrometer (QCLS). *Atmospheric Measurement Techniques*, *9*(11), 5293–5314. https://doi.org/10.5194/amt-9-5293-2016

Le Quéré, C., Andrew, R., Friedlingstein, P., Sitch, S., Hauck, J., Pongratz, J., … Zheng, B. (2018). Global Carbon Budget 2018. *Earth System Science Data*, *10*(4), 2141–2194. https://doi.org/10.5194/essd-10-2141-2018

Linder, S., & Troeng, E. (1980). Photosynthesis and Transpiration of 20-Year-Old Scots Pine. *Ecological Bulletins*, (32), 165–181.

Maseyk, K., Berry, J. A., Billesbach, D., Campbell, J. E., Torn, M. S., Zahniser, M., & Seibt, U. (2014). Sources and sinks of carbonyl sulfide in an agricultural field in the Southern Great Plains. *Proceedings of the National Academy of Sciences of the United States of America*, *111*(25), 9064–9069. https://doi.org/10.1073/pnas.1319132111

Montzka, S. A., Calvert, P., Hall, B. D., Elkins, J. W., Conway, T. J., Tans, P. P., & Sweeney, C. S. (2007). On the global distribution, seasonality, and budget of atmospheric carbonyl sulfide (COS) and some similarities to CO2. *Journal of Geophysical Research Atmospheres*, *112*(9), 1–15. https://doi.org/10.1029/2006JD007665

Pearson, K. (1895). Notes on regression and inheritance in the case of two parents. In *Proceedings of the Royal Society of London* (58th ed., pp. 240–263).

Rautiainen, M., Heiskanen, J., & Korhonen, L. (2012). Seasonal changes in canopy leaf area index and MODIS vegetation products for a boreal forest site in central Finland Seasonal changes in canopy leaf area index and MODIS vegetation products for a boreal forest site in central Finland. *Boreal Environmental Research*, *17*, 72–84.

Reichstein, M., Falge, E., Baldocchi, D., Papale, D., Aubinet, M., Berbigier, P., … Valentini, R. (2005). On the separation of net ecosystem exchange into assimilation and ecosystem respiration: Review and improved algorithm. *Global Change Biology*, *11*(9), 1424–1439. https://doi.org/10.1111/j.1365-2486.2005.001002.x

Ronda, R. J., De Bruin, H. A. R., & Holtslag, A. A. M. (2001). Representation of the canopy conductance in modeling the surface energy budget for low vegetation. *Journal of Applied Meteorology*, *40*(8), 1431–1444. https://doi.org/10.1175/1520-0450(2001)040<1431:ROTCCI>2.0.CO;2

Sander, R. (2015). Compilation of Henry's law constants (version 4.0) for water as solvent. *Atmospheric Chemistry and Physics*, *15*, 4399–4981. https://doi.org/10.5194/acp-15-4399-2015

Sandoval-Soto, L., Stanimirov, M., Hobe, M. Von, Schmitt, V., Valdes, J., Wild, A., & Kesselmeier, J. (2005). Global uptake of carbonyl sulfide (COS) by terrestrial vegetation : Estimates corrected by deposition velocities normalized to the uptake of carbon dioxide (CO2). *Biogeosciences*, *2*, 125–132. https://doi.org/https://doi.org/10.5194/bg-2-125-2005

Schulze, D.-E., Kelliher, F. M., Körner, C., Lloyd, J., & Leuning, R. (1994). Relationships among Maximum Stomatal Conductance, Ecosystem Surface Conductance, Carbon Assimilation Rate, and Plant Nitrogen Nutrition: A Global Ecology Scaling Exercise. *Annual Review of Ecology and Systematics*,

25(1), 629–660.
Seibt, U., Kesselmeier, J., Sandoval-Soto, L., Kuhn, U., & Berry, J. A. (2010). A kinetic analysis of leaf uptake of COS and its relation to transpiration, photosynthesis and carbon isotope fractionation. *Biogeosciences*, *7*(1), 333–341. https://doi.org/10.5194/bg-7-333-2010
Spearman, C. (1904). The Proof and Measurement of Association between Two Things Author (s): C . Spearman Source : The American Journal of Psychology , Vol . 15 , No . 1 (Jan ., 1904), pp . 72-101 Published by : University of Illinois Press Stable URL : https://www.jstor. *The American Journal of Psychology*, *15*(1), 72–101.
Stimler, K., Berry, J. A., & Yakir, D. (2012). Effects of carbonyl sulfide and carbonic anhydrase on stomatal conductance. *Plant Physiology*, *158*(1), 524–530. https://doi.org/10.1104/pp.111.185926
Stimler, K., Montzka, S. A., Berry, J. A., Rudich, Y., & Yakir, D. (2010). Relationships between carbonyl sulfide (COS) and CO2 during leaf gas exchange. *New Phytologist*, *186*(4), 869–878. https://doi.org/10.1111/j.1469-8137.2010.03218.x
Sun, W., Kooijmans, L. M. J., Maseyk, K., Chen, H., Mammarella, I., Vesala, T., … Seibt, U. (2018). Soil fluxes of carbonyl sulfide (COS), carbon monoxide, and carbon dioxide in a boreal forest in southern Finland. *Atmospheric Chemistry and Physics*, *18*(2), 1363–1378. https://doi.org/10.5194/acp-18-1363-2018
Sun, W., Maseyk, K., Lett, C., & Seibt, U. (2015). A soil diffusion-reaction model for surface COS flux: COSSM v1. *Geoscientific Model Development*, *8*(10), 3055–3070. https://doi.org/10.5194/gmd-8-3055-2015
Vilà-Guerau de Arellano, J., Gioli, B., Miglietta, F., Jonker, H. J. J., Baltink, H. K., Hutjes, R. W. A., & Holtslag, A. A. M. (2004). Entrainment process of carbon dioxide in the atmospheric boundary layer. *Journal of Geophysical Research Atmospheres*, *109*(18), 1–16. https://doi.org/10.1029/2004JD004725
Wang, K., Kellomäki, S., & Laitinen, K. (1995). Effects of needle age , long-term temperature and CO 2 treatments on the photosynthesis of Scots pine. *Tree Physiology*, *15*, 211–218.
Wesely, M. L. (1989). Parameterization of surface resistances to gaseous dry deposition in regional-scale numerical models. *Atmospheric Environment*, *23*, 1293–1304. https://doi.org/10.1016/j.atmosenv.2007.10.058
Whelan, M. E., Lennartz, S. T., Gimeno, T. E., Wehr, R., Wohlfahrt, G., Wang, Y., … Elliott Campbell, J. (2018). Reviews and syntheses: Carbonyl sulfide as a multi-scale tracer for carbon and water cycles. In *Biogeosciences* (Vol. 15). https://doi.org/10.5194/bg-15-3625-2018
Wohlfahrt, G., Brilli, F., Hörtnagl, L., Xu, X., Bingemer, H., Hansel, A., & Loreto, F. (2012). Carbonyl sulfide (COS) as a tracer for canopy photosynthesis, transpiration and stomatal conductance: Potential and limitations. *Plant, Cell and Environment*, *35*(4), 657–667. https://doi.org/10.1111/j.1365-3040.2011.02451.x
Yanez-Serrano, A. M., Christine Nölscher, A., Bourtsoukidis, E., Gomes Alves, E., Ganzeveld, L., Bonn, B., … Andreae, M. O. (2018). Monoterpene chemical speciation in a tropical rainforest: variation with season, height, and time of dayat the Amazon Tall Tower Observatory (ATTO). *Atmospheric Chemistry and Physics*, *18*(5), 3403–3418. https://doi.org/10.5194/acp-18-3403-2018
Yang, F., Qubaja, R., Tatarinov, F., Stern, R., & Yakir, D. (2019). Soil-atmosphere exchange of carbonyl sulfide in a Mediterranean citrus orchard. *Atmospheric Chemistry and Physics*, *19*(6), 3873–3883. https://doi.org/10.5194/acp-19-3873-2019
Zhao, S., Yi, H., Tang, X., Jiang, S., Gao, F., Zhang, B., … Wang, Z. (2013). The Hydrolysis of Carbonyl Sulfide at Low Temperature: A Review. *The Scientific World Journal*, *2013*, 1–8.

Appendix A - Model edits:

Here the edits made to MLC-CHEM are summarised as used for the final model settings. The numbers in front of the code represent the line numbers in the file.

Messy_emdp_xtsurf.f90:

Increased the minimum prahveg to 10 to prevent extremely high Kh values:

```
285     prahveg(jl)=MAX(10._dp,(1./(pustveg(jl)*ckap))* &
286           (LOG((geopot_3d(jl)/g)/ &
287           MAX(0.02_dp,z0m(jl)))-psih(jl)))
```

Added variable COS mesophyll conductance using COS stomatal conductance

```
796     IF (l_xtsurf_AGS.AND.jt.EQ.idt_COS) THEN
797               rmesophyll(jt)=(rco_leaf(jl,2)*diff(jt))*2.6
798               print *, jl, jt, rmesophyll(jt), rco_leaf(jl,6)
799     ENDIF
```

Added and changed COS specific parameters relating to stomatal and non-stomatal uptake.

```
2090    IF (TRIM(trname(jt))=='COS') THEN
2091          rws(jt)=1e5_dp
2092          rmes(jt)=4.7e3_dp
2093          rsoil(jt)=5.1e3_dp
2094          diffrb(jt)=1.5_dp
2095          diff(jt)=2._dp
2096    ENDIF
```

A-g_s model (within messy_emdep_xtsurf.f90):

Changes made to the A-g_s model, see for all final settings of the A-g_s model Appendix B

```
4852    CGM25(3)=1.0          Was originally set to 7, see Linder & Troeng, 1980
4892    CF0(3)=.85            Was originally set to 0.90 (Seibt et al., 2010 give value of 0.71)
4919    CAMAX25(3)=1.         Was originally set to 0.45, Schultze et al., 1994 and Wang et al., 1995
```

Messy_emdep_xtsurf_box.f90:

Added hyytiälä 2015 to scaling of length of day used for mixed layer depth calculation.

```
849     IF (casename.EQ.'Hyytiala, 2010'.OR.casename.EQ.'Hyytiala, 2015') THEN
850        scaling =   MAX(0.,COS ((15./360)*(timeday(i)-(12+doffset))*1.25*PI))
```

Changes to and new measurement input loaded from the input file:

Input for measured relative humidity

```
1629    IF (observ(i,10) > 0.) rh(i)=observ(i,10)
```

Input for measured CO_2 and O_3 mixing ratios

```
1648    IF(observ(i,14) > 0.)   pxtm1_obs(i,idt_CO2)=1e-6*observ(i,14)
1649    IF(observ(i,14) > 0.)   pxtm1_obs(i,idt_O3)=1e-9*observ(i,17)
```

Input for measured friction velocity (u)*

```
1651     IF (observ(i,11) > -4000.) zustveg(i) = observ(i,11)
```

Input of CO_2 soil flux – calculated from soil temperature

```
1653     IF (observ(i,15) > 0.) co2_slflux(i)=1e-6*(-1.0065+exp(0.1300*(tsoil(i)-273.15)))*avo
```

Included COS in tendencies output file (by replacing HONO)

Line 2801 to Line 3114 → Where tendencies for HONO were written to output file these are now replaced by COS to be able to observe COS tendencies.

Increased O_3 mixing ratio for when measured data was not available (was originally 15)

```
3773     IF (trname(i) == 'O3      ') pxtm1(:,i)=30.e-9_dp
```

Increased COS mixing ratio for when measured data was not available

```
3783     IF (trname(i) == 'COS     ') pxtm1(:,i)=420.e-12_dp
```

Appendix B – Final A-g_s settings

Here the final settings used for the A-g_s model are shown including the changes made as shown in Appendix A.

Table B1: Final A-g_s model settings. Columns indicated in yellow are changed compared to original settings

	Original value	New value
CGAMMA25	45	45
CGAMMAQ10	1.5	1.5
CGM25	7	1
CGMQ10	2	2
CGMT1	5	5
CGMT2	28	28
CGC	0.25	0.25
CF0	0.90	0.80
CRICO	-0.15	-0.15
CEPSILON0	0.17	0.17
CAMAX25	0.45	1
CAMAXQ10	2	2
CAMAXT1	8	8
CAMAXT2	38	38